



Chronus: Understanding and Securing the Cutting-Edge Industry Solutions to DRAM Read Disturbance

Oğuzhan Canpolat^{§†} A. Giray Yağlıkçı[§] Geraldo F. Oliveira[§] Ataberk Olgun[§]
 Nisa Bostancı[§] Ismail Emir Yuksel[§] Haocong Luo[§] Oğuz Ergin^{‡†} Onur Mutlu[§]
[§]ETH Zürich [†]TOBB University of Economics and Technology [‡]University of Sharjah

Read disturbance in modern DRAM is an important robustness (security, safety, and reliability) problem, where repeatedly accessing (hammering) a row of DRAM cells (DRAM row) induces bitflips in other physically nearby DRAM rows. Shrinking technology node size exacerbates DRAM read disturbance over generations. To help mitigate read disturbance, the latest DDR5 specifications (as of April 2024) introduced a new RowHammer mitigation framework, called Per Row Activation Counting (PRAC). PRAC 1) enables the DRAM chip to accurately track row activations by allocating an activation counter per row and 2) provides the DRAM chip with the necessary time window to perform RowHammer-preventive refreshes by introducing a new back-off signal. Unfortunately, no prior work rigorously studies PRAC's security guarantees and overheads. In this paper, we 1) present the first rigorous security, performance, energy, and cost analyses of PRAC and 2) propose Chronus, a new mechanism that addresses PRAC's two major weaknesses.

Our analysis shows that PRAC's system performance overhead on benign applications is non-negligible for modern DRAM chips and prohibitively large for future DRAM chips that are more vulnerable to read disturbance. We identify two weaknesses of PRAC that cause these overheads. First, PRAC increases critical DRAM access latency parameters due to the additional time required to increment activation counters. Second, PRAC performs a constant number of preventive refreshes at a time, making it vulnerable to an adversarial access pattern, known as the wave attack, and consequently requiring it to be configured for significantly smaller activation thresholds.

To address PRAC's two weaknesses, we propose a new on-DRAM-die RowHammer mitigation mechanism, Chronus. Chronus 1) updates row activation counters concurrently while serving accesses by separating counters from the data and 2) prevents the wave attack by dynamically controlling the number of preventive refreshes performed. Our performance analysis shows that Chronus's system performance overhead is near-zero for modern DRAM chips and very low for future DRAM chips. Chronus outperforms three variants of PRAC and three other state-of-the-art read disturbance solutions. We discuss Chronus's and PRAC's implications for future systems and foreshadow future research directions. To aid future research, we open-source our Chronus implementation at <https://github.com/CMU-SAFARI/Chronus>.

1. Introduction

To ensure system robustness (security, safety, and reliability), it is critical to maintain memory isolation: accessing a mem-

ory address should *not* cause unintended side-effects on data stored in other addresses [1]. Unfortunately, with aggressive technology scaling, DRAM [2], the prevalent main memory technology, suffers from increased *read disturbance*: accessing (reading) a row of DRAM cells (i.e., a DRAM row) degrades the data integrity of other physically close but *unaccessed* DRAM rows. RowHammer [1] is a prime example of DRAM read disturbance, where a row (i.e., victim row) can experience bitflips when at least one nearby row (i.e., aggressor row) is repeatedly activated (i.e., hammered) [1, 13, 38, 45, 49, 53, 68, 82–142] more times than a threshold, called the *minimum hammer count to induce the first bitflip* (N_{RH}). RowPress [143] is another prime example of DRAM read disturbance that amplifies the effect of RowHammer by keeping an aggressor row open for longer, thereby causing more disturbance with each activation and consequently reducing N_{RH} .

A simple way of mitigating DRAM read disturbance is to preventively refresh potential victim rows before bitflips occur. Unfortunately, a preventive refresh blocks accesses to thousands of DRAM rows that are in the same DRAM bank for a non-negligible time window (e.g., 350ns [144]), in which the memory controller should *not* issue any other DRAM command to the bank. As DRAM chips become more vulnerable to read disturbance with technology node scaling, preventive refreshes can significantly reduce system performance [1, 4–7, 11, 17, 20–22, 24, 35, 42, 44, 47–49, 55, 59, 68, 79, 145–147]. Therefore, it is important to accurately identify when a preventive refresh is needed and perform it in a timely manner.

To provide DRAM chips with the necessary flexibility to perform preventive refreshes in a timely manner, recent DRAM standards (e.g., DDR5 [144, 148]) introduce 1) a command called *refresh management (RFM)* [148] and 2) a framework called *Per Row Activation Counting (PRAC)* [144]. RFM is a command that provides the DRAM chip with a time window (e.g., 195 ns [144]) to perform preventive refreshes. Specifications before 2024 (e.g., earlier DDR5 [148]) advise the memory controller to issue RFM when the number of row activations in a bank or a logical memory region exceeds a threshold (e.g., 32 [144]), a mechanism we call *periodic RFM (PRFM)*.

A recent update (as of April 2024) of the JEDEC DDR5 specification [144, 149] introduces a new on-DRAM-die read disturbance mitigation framework called PRAC. PRAC has two key features. First, PRAC maintains an activation counter per DRAM row [1] to accurately identify when a preventive refresh is needed. PRAC increments a DRAM row's activation counter

while the row is being closed, which increases the latency of closing a row, i.e., the precharge latency (t_{RP}) and row cycle time (t_{RC}) timing parameters. Second, PRAC proposes a new *back-off* signal to convey the need for preventive refreshes from the DRAM chip to the memory controller, similar to what prior works propose [5, 9, 20, 36, 147, 150]. The DRAM chip asserts this back-off signal when a DRAM row’s activation count reaches a critical value. Within a predefined time window (e.g., 180 ns [144]) after receiving the back-off signal, the memory controller has to issue an RFM command so that the DRAM chip can perform the necessary preventive refresh operations. PRAC aims to 1) avoid read disturbance bitflips by performing necessary preventive refreshes in a timely manner and 2) minimize unnecessary preventive refreshes by accurately tracking each row’s activation count. Unfortunately, *no* prior work rigorously investigates PRAC’s security, performance, energy, and storage cost implications for modern and future systems.

In this paper, we 1) present the first rigorous security, performance, energy, and storage cost analyses of PRAC, which identifies PRAC’s two major weaknesses and 2) propose a new mechanism, Chronus, which addresses those weaknesses.

PRAC Analysis. We analyze PRAC in three steps. First, we define a security-oriented adversarial access pattern that achieves the highest possible activation count in systems protected by PRAC. Second, we conduct a security analysis by evaluating the highest possible activation count that a DRAM row can reach under different configurations of PRAC. Our security analysis shows that PRAC can be configured for secure operation against an N_{RH} value of 20 or higher. Third, we conduct a system performance analysis using cycle-accurate simulations with an open-source simulator, Ramulator 2.0 [151, 152]. Our system performance results across 60 different four-core multi-programmed workload mixes show that: At modern N_{RH} values higher than 1K, PRAC’s overheads are mainly dominated by the increased critical DRAM timing parameters where PRAC incurs high average (maximum) 5.8% (8.9%) system performance and 10.7% (13.5%) DRAM energy overheads. For the lowest secure N_{RH} value of 20, these overheads increase to 78.5% (90.7%) and 6.6x (7.1x), respectively.¹

We attribute these large overheads to two key weaknesses in PRAC. First, PRAC increases critical DRAM timing parameters due to the additional time required to increment activation counters. Second, PRAC performs a fixed number of preventive refreshes at a time and enforces a *delay period* during which preventive refreshes *cannot* be requested, making it vulnerable to an adversarial access pattern known as the *wave attack*.

Chronus. To address PRAC’s two major weaknesses, we propose Chronus. Chronus 1) updates row activation counters *concurrently* while serving accesses by physically separating

¹Our analysis rigorously sweeps N_{RH} to extremely low values (e.g., 20). This is because a mitigation mechanism that securely scales to low N_{RH} values with low performance and energy overheads provides two benefits: 1) activation counters maintain fewer bits, resulting in smaller hardware complexity and 2) read disturbance profiling becomes significantly shorter as each DRAM row can be tested for a smaller hammer count (e.g., hammering the row 64 times takes $16\times$ shorter than hammering the row 1024 times).

counters from the data and 2) prevents the wave attack by dynamically controlling the number of preventive refreshes performed by the memory controller and removing the delay period after the memory controller performs preventive refreshes.²

Key Results. We compare Chronus to 1) three variants of PRAC, as the state-of-the-art industry solutions, and 2) three other state-of-the-art academic proposals, i.e., Graphene [4], Hydra [24], and PARA [1]. Our performance analysis shows that Chronus outperforms *all* six evaluated mechanisms across all studied workloads and N_{RH} values. Chronus incurs near-zero system performance ($<0.1\%$ on average) and relatively low (compared to PRAC) DRAM energy (10.3% on average) overheads for modern DRAM chips ($N_{RH} = 1K$) and low system performance (8.3% on average) and DRAM energy (17.9% on average) overheads for future DRAM chips ($N_{RH} = 20$).

We make the following contributions:

- We present the first security analysis of industry’s state-of-the-art read disturbance solution, PRAC, and provide robust configurations against its worst-case access pattern.
- We rigorously evaluate the performance, energy, and cost implications of PRAC’s different configurations for modern and future DRAM chips. Our results show that PRAC incurs non-negligible overheads due to two major weaknesses: 1) increased critical DRAM timing parameters, and 2) wave attack vulnerability due to allowing only a fixed number of preventive refreshes.
- We propose Chronus, which addresses the weaknesses of PRAC through 1) updating row activation counters concurrently while serving accesses by separating counters from the data and 2) preventing wave attacks by dynamically controlling the number of preventive refreshes as needed. We show that Chronus’s system performance overhead is near-zero (very low) for modern (future) DRAM chips.
- We compare Chronus against three variants of PRAC and three state-of-the-art mitigation mechanisms. Our results show that 1) Chronus outperforms all evaluated mitigation mechanisms at all evaluated N_{RH} values and 2) PRAC variants underperform against three of the four (including Chronus) mitigation mechanisms for modern DRAM chips with relatively high (i.e., $\geq 1K$) N_{RH} values.
- To aid future research in a transparent manner, we open-source our implementations with Ramulator 2.0 [154].

2. Background

2.1. DRAM Organization and Operation

Organization. Fig. 1 shows the hierarchical organization of a modern DRAM-based main memory. The memory controller connects to a DRAM module over a memory channel. A module contains one or multiple DRAM ranks that time-share the memory channel. A rank consists of multiple DRAM chips.

²In Greek mythology, Cronus is renowned for separating heaven and earth [153], and Chronos for controlling time [153]. We chose their blended name, Chronus, which resembles our proposal: separating counters (similar to Cronus separating worlds) and dynamically controlling the number of preventive refreshes (similar to Chronos controlling time).

Each DRAM chip has multiple DRAM banks each of which contains multiple subarrays. A DRAM bank is organized as a two-dimensional array of DRAM cells, where a row of cells is called a DRAM row. A DRAM cell consists of 1) a storage capacitor, which stores one bit of information in the form of electrical charge, and 2) an access transistor.

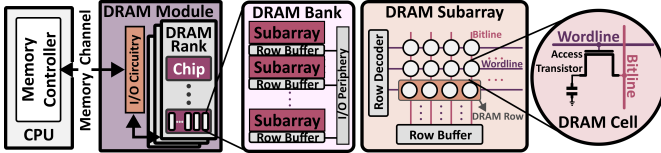


Figure 1: DRAM organization

Operation. To access a DRAM row, the memory controller issues a set of commands to DRAM over the memory channel. The memory controller sends an *ACT* command to activate a DRAM row, which asserts the corresponding wordline and loads the row data into the row buffer. Then, the memory controller can issue *RD*/*WR* commands to read from/write into the DRAM row. An access to the row that is already in the row buffer causes a row hit. To access a different row, the memory controller must first close the opened row and prepare the bank for a new activation by issuing a *PRE* command. Therefore, accessing a different row from the one in the row buffer causes a row conflict in the row buffer.

DRAM cells are inherently leaky and lose their charge over time due to charge leakage in the access transistor and the storage capacitor. To maintain data integrity, the memory controller periodically refreshes each row in a time interval called refresh window (t_{REFW}) (32ms for DDR5 [155] and 64ms for DDR4 [156]). To ensure all rows are refreshed every t_{REFW} , the memory controller issues *REF* commands with a time interval called refresh interval (t_{REFI}) (3.9 μ s for DDR5 [155] and 7.8 μ s for DDR4 [156]).

Timing Parameters. To ensure correct operation, the memory controller must obey specific timing parameters while accessing DRAM. In addition to t_{REFW} and t_{REFI} , we explain three timing parameters related to the rest of the paper: i) the minimum time interval between two consecutive *ACT* commands targeting the same bank (t_{RC}), ii) the minimum time needed to issue a *PRE* command following an *ACT* command (t_{RAS}), and iii) the minimum time needed to issue an *ACT* command following a *PRE* command (t_{RP}). Detailed explanations of these parameters can be found in [157–159].

2.2. DRAM Read Disturbance

As DRAM manufacturing technology node size shrinks, interference across rows increases, exacerbating circuit-level read disturbance mechanisms. Two prime examples of read disturbance mechanisms are RowHammer [1] and RowPress [143], where repeatedly activating (i.e., hammering) a DRAM row (i.e., aggressor row) or keeping the aggressor row active for a long time (i.e., pressing) induces bitflips in physically nearby rows (i.e., victim rows), respectively. To induce read disturbance bitflips, 1) an aggressor row needs to be hammered more than a threshold value called N_{RH} [1] or 2) an aggressor needs to be pressed

for long enough [135–137, 143]. Various characterization studies [1, 13, 30, 38, 49, 62, 76, 103, 110, 121, 124, 129–143, 160–171] show that as DRAM technology scaling continues to smaller technology node sizes, DRAM chips are becoming more vulnerable to read disturbance (i.e., newer chips have lower N_{RH} values). For example, one can induce RowHammer bitflips by activating two aggressors that are physically adjacent to a victim row (i.e., double-sided RowHammer) 4.8K times each in the chips manufactured in 2020 while a row needs to be hammered 69.2K times in older chips manufactured in 2013 [135]. To make matters worse, RowPress [143] reduces N_{RH} by 1-2 orders of magnitude.

DRAM Read Disturbance Mitigation Mechanisms. Many prior works propose mitigation techniques [1, 3–26, 30, 31, 35–38, 40–51, 53, 55–81, 147, 156, 172–175] to protect DRAM chips against RowHammer bitflips leveraging different approaches. These mechanisms perform two tasks: 1) execute a trigger algorithm and 2) perform preventive actions. The trigger algorithm observes the memory access patterns and triggers a preventive action based on the result of a probabilistic or a deterministic process. The preventive action is one of 1) preventively refreshing victim row [1, 4–7, 11, 17, 20–22, 24, 35, 42, 44, 47–49, 55, 59, 68, 79, 145–147], 2) dynamically remapping aggressor rows [3, 12, 57, 69], and 3) throttling unsafe accesses [18, 19]. Existing RowHammer mitigation mechanisms can also prevent RowPress bitflips when their trigger algorithms are configured to be more aggressive, which is practically equivalent to configuring them for sub-1K N_{RH} values [143]. Unfortunately, existing RowHammer mitigation mechanisms incur prohibitively large performance overheads at low N_{RH} values (i.e., sub-1K) because they more aggressively perform preventive actions. Given that DRAM read disturbance worsens with shrinking technology node size, N_{RH} values are expected to reduce even more [1, 34, 136]. Therefore, reducing the performance overhead of existing RowHammer mitigation mechanisms is critical.

PRAC. Various prior works discuss the use of per-row activation counters to detect how many times each row in DRAM is activated within a refresh interval [1, 36, 47, 61, 147]. A recent update (as of April 2024) of the JEDEC DDR5 specification [144, 149] introduces a similar on-DRAM-die read disturbance mitigation mechanism called PRAC (explained in §3), which aims to ensure robust operation at low overhead by preventively refreshing victim rows when necessary. Although PRAC is a promising DRAM specification advancement, *no* prior work rigorously analyzes PRAC’s impact on security, performance, energy, and cost for modern and future systems.³

3. A Brief Summary of RFM and PRAC

This section briefly explains the RFM command, PRAC mechanism, and assumptions we use for our evaluations.

RFM Command. RFM is a DRAM command that provides the DRAM chip with a time window (e.g., 195 ns [144]) so that the DRAM chip can preventively refresh potential victim rows. The DRAM chip is responsible for identifying and preventively

³An earlier version of this paper was presented at DRAMSec 2024 [176].

refreshing potential victim rows, and the memory controller is responsible for issuing RFM commands.

PRAC Overview. PRAC [144], as described in the JEDEC DDR5 standard updated in April 2024 [144], implements an activation counter for each DRAM row, and thus accurately measures the activation counts of *all* rows. When a row’s activation count reaches a threshold, the DRAM chip asserts a back-off signal which forces the memory controller to issue an RFM command. The DRAM chip preventively refreshes potential victim rows upon receiving an RFM command.

Assumptions About PRAC. We make two assumptions: 1) PRAC always refreshes victims of the row with the maximum activation count during each RFM command and 2) physically-adjacent DRAM rows can experience bitflips when a DRAM row is activated at least N_{RH} times.

PRAC’s Operation and Parameters. PRAC increments a row’s activation count during a precharge command. When a bank receives a precharge command, the bank internally reads, modifies, and writes the open row’s counter before de-asserting the wordline. As such, PRAC’s counter update affects several DRAM timing parameters around row accesses. Table 1 summarizes DRAM timing parameter changes when PRAC is enabled for the DRAM 3200AN [144] speed bin.

Table 1: DRAM Timing Parameter Changes with PRAC

Parameter	Description	DDR5	DDR5
		without PRAC	with PRAC
t_{RAS}	minimum time for a <i>PRE</i> after an <i>ACT</i> to the same bank	32 ns	16 ns
t_{RP}	minimum time for an <i>ACT</i> after a <i>PRE</i> to the same bank	15 ns	36 ns
t_{RC}	minimum time for two <i>ACT</i> s to the same bank	47 ns	52 ns
t_{RTP}	minimum time for a <i>PRE</i> after a <i>RD</i> to the same bank	7.5 ns	5 ns
t_{WR}	minimum time for a <i>PRE</i> after a <i>WR</i> to the same bank	30 ns	10 ns

We make two observations from Table 1. First, the t_{RP} and t_{RC} timing parameters increase because of the additional time needed to update the counter before the wordline is de-asserted. Second, the t_{RAS} , t_{RTP} , and t_{WR} timing parameters likely reduce to account for the additional time the row stays open as the counter is updated. We note that PRAC timing parameters can also be better utilizing the aggressive guardbands existing in modern DRAM chips as shown in [137, 159, 177–182] to reduce one or more of the latter three timing parameters.

The DRAM chip asserts the back-off signal when a row’s activation count reaches a fraction of N_{RH} , denoted as the back-off threshold (N_{BO}), where the fraction can be configured to either 70%, 80%, 90%, or 100% [144]. The memory controller receives the back-off signal shortly after (e.g., ≈ 5 ns [144]) issuing a precharge (PRE) command. The memory controller and the DRAM chip go through three phases when the back-off signal is asserted. First, during *the window of normal traffic* (t_{ABOACT}) [144], the memory controller has a limited time window (e.g., 180 ns [144]) to serve requests after receiving the back-off signal. A DRAM row can receive up to t_{ABOACT}/t_{RC}

activations in this window. Second, during the *recovery period* [144], the memory controller issues a number of RFM commands, which we denote as N_{Ref} (e.g., 1, 2 or 4 [144]). An RFM command can further increment the activation count of a row before its potential victims are refreshed. Third, during the *delay period* or the delay until a new back-off can be initiated ($t_{BackOffDelay}$) [144], the DRAM chip *cannot* reassert the back-off signal until it receives a number of activate commands, which we denote as N_{Delay} (e.g., 1, 2 or 4 [144]).⁴ Taking into account these three phases, §5 calculates the highest achievable activation count to any row in a PRAC-protected system.

Determining Rows to Refresh During an RFM Command.

PRAC maintains a large number of counters in each DRAM bank. As such, it is *not* practical for the DRAM bank to search for the row with the maximum activation count during an RFM command. To track the rows with the highest activation counts, our PRAC implementation uses a relatively small per-bank table (e.g., 4 entries store enough rows for each RFM command to refresh during the recovery period) that we call the *Aggressor Tracking Table* (ATT). The table starts empty (i.e., all entries are invalid). When a row is precharged, the table is updated with the precharged row’s counter value if 1) the precharged row exists in the table, 2) an entry in the table is invalid, or 3) the precharged row’s counter value exceeds the table entry with the *lowest* activation count. When a DRAM bank receives an RFM command, the bank invalidates and refreshes the potential victims of the table entry with the *maximum* activation count.

RFM and PRAC Implementations. We analyze three different RFM and PRAC implementations: 1) *Periodic RFM (PRFM)*, where the memory controller issues an RFM command *periodically* when the total number of activations to a bank reaches a predefined threshold called *bank activation threshold to issue an RFM command* (RFM_{th}) with *no* back-off signal from the DRAM chip, as described in early DDR5 standards [148]; 2) *PRAC-N*, where the memory controller issues N back-to-back RFM commands *only* after receiving a back-off signal from the DRAM chip, as described in the latest JEDEC DDR5 standard [144, 149]; 3) *PRAC+PRFM*, where the memory controller issues an RFM command when *i*) the total number of activations to a bank reaches $RFM_{th} = 75$ or *ii*) it receives a back-off signal from the DRAM chip.⁵ As shown in §5, PRAC-N implementations are *not* secure at N_{RH} values lower than 20. Therefore, combining PRAC and PRFM enables security at lower N_{RH} values at the cost of potentially refreshing the victims of aggressor rows whose activation counts are *not* close to N_{RH} .

4. Adversarial Access Pattern: The Wave Attack

We describe our threat model and the adversarial access pattern, known as *the wave attack* [20, 147] or *the feinting attack* [35].

Threat Model. We assume that the attacker 1) knows the physical layout of DRAM rows (as in [18]), 2) accurately detects

⁴Current DDR5 specification [144] notes that N_{Ref} and N_{Delay} always have the same value. To comprehensively assess PRAC’s security guarantees, we also consider different values in our security analysis (§5).

⁵The RFM_{th} of 75 is provided in the example PRAC+PRFM configuration in the latest (as of April 2024) JEDEC DDR5 standard [144].

when a row is internally refreshed (preventively or periodically, as in U-TRR [68]), and 3) precisely times *all* DRAM commands except refresh (REF) and RFM commands (as in [18, 68]).

Overview. The wave attack aims to achieve the highest activation count for a given row in an RFM and PRAC-protected DRAM chip by overwhelming the mitigation mechanism using a number of decoy rows. Fig. 2 visualizes the buildup of a wave attack against a periodic read disturbance mitigation mechanism (e.g., PRFM) that refreshes the potential victims of an aggressor for every three row activations.

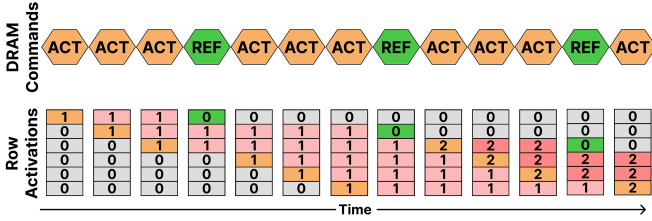


Figure 2: Wave attack buildup visualization

In this access pattern, the attacker hammers several rows in a balanced manner, such that the mitigation mechanism can perform preventive refreshes *only* for a small subset of the hammered rows when a preventive refresh is issued. When an aggressor row’s victims are refreshed, the attacker excludes the aggressor row in the next round of activations. By doing so, this adversarial access pattern achieves the highest possible activation count for the row whose victims are preventively refreshed last. More details and analyses of the attack can be found in [20, 35, 147].

5. Configuration of PRAC and Security Analysis

This section investigates different RFM and PRAC configurations and their impact on security under the wave attack.

Key Parameters. We assume a *blast radius* of 2 [120], a t_{RC} of 52 ns [144], and a refresh management latency (t_{RFM}) of 350 ns [144], which allows an RFM command to refresh four victim rows of one aggressor row.

Notation. R_i is the set of rows that the wave attack hammers in round i and $|R_i|$ is the number of rows in R_i .

PRFM. In round 1, the wave attack hammers each row in R_1 once, causing the memory controller to issue $\lfloor (|R_1|/RFM_{th}) \rfloor$ RFM commands, each refreshing four victims of one aggressor row. In round 2, the wave attack hammers the non-mitigated rows R_2 , where $|R_2| = |R_1| - \lfloor (|R_1|/RFM_{th}) \rfloor$. By repeating this calculation i times, Equation 1 evaluates the number of non-mitigated rows at an arbitrary round i ($|R_i|$).

$$|R_i| = |R_1| - \left\lfloor \frac{\sum_{k=1}^{i-1} |R_k|}{RFM_{th}} \right\rfloor \quad (1)$$

To cause bitflips, the wave attack must make sure that 1) at least one aggressor row is not mitigated (i.e., its victims are *not* refreshed by an RFM command until the end of round N_{RH} , i.e., $|R_{N_{RH}}| > 0$), and 2) the time taken by the attacker’s row activations and RFM preventive refreshes do *not* exceed t_{REFW} , i.e., aggressor’s victims are *not* periodically refreshed before being activated N_{RH} times. We rigorously sweep the

wave attack’s parameters and identify the maximum hammer count of an aggressor row before its victims are refreshed.

PRAC-N. We adapt our PRFM wave attack analysis to PRAC-N by leveraging two key insights. First, PRAC-N mechanism will *not* preventively refresh any row until a row’s activation count reaches N_{BO} (i.e., the back-off threshold). We prepare rows in R_1 such that each row is already hammered $N_{BO}-1$ times. Doing so, the number of rounds necessary to induce a bitflip is reduced by $N_{BO}-1$. Second, at least one row’s activation counter remains above N_{BO} across *all* rounds after initialization until the end of the wave attack. This causes PRAC-N to assert the back-off signal as frequently as possible, i.e., with a time period containing a recovery period ($N_{Ref} \times t_{RFM}$), a delay period ($t_{BackOffDelay}$), and a window of normal traffic (t_{ABOACT}) [144]. Leveraging these insights, we update Equation 1 to derive Equation 2.

$$|R_i| = |R_1| - N_{Ref} \times \left\lfloor \frac{\sum_{k=1}^{i-1} |R_k|}{(N_{Delay} + (t_{ABOACT}/t_{RC}))} \right\rfloor \quad (2)$$

For a PRAC-N system to be secure, an attacker should *not* be able to obtain $|R_{N_{RH}-N_{BO}}| > 0$ within t_{REFW} for any R_1 . We analyze the maximum hammer count of an aggressor row before its victims are refreshed in a PRAC-N-protected system for a wide set of N_{BO} and $|R_1|$ configurations.

Configuration Sweep. Fig. 3 shows the maximum activation count an aggressor row can reach before its victims are refreshed (y-axis) for PRFM and PRAC-N in Figs. 3a and 3b, respectively. Fig. 3a shows the bank activation threshold to issue an RFM command (RFM_{th}) on the x-axis and starting (i.e., round 1) row set size ($|R_1|$) color-coded. Fig. 3b shows the back-off threshold (N_{BO}) on the x-axis and N_{Ref} color-coded. In Fig. 3b, each bar depicts the *worst-case* starting row set size (i.e., $|R_1|$ that yields the highest activation count).

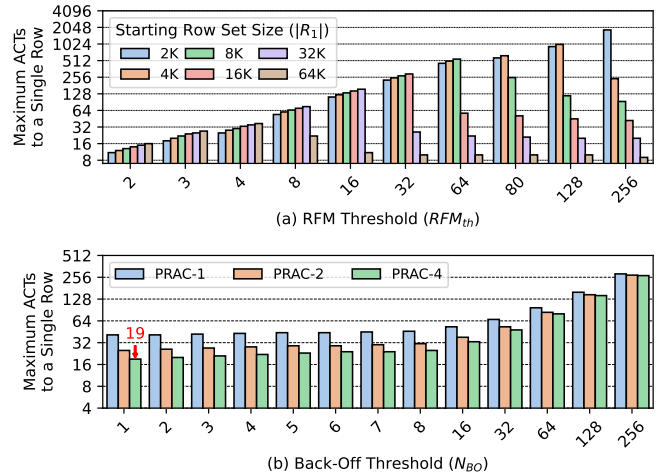


Figure 3: Maximum activations to a row allowed by (a) PRFM and (b) PRAC-N

From Fig. 3a, we observe that to prevent bitflips for very low N_{RH} values (e.g., 32 on the y axis), RFM_{th} should be configured to very low values (e.g., < 4), as only such RFM_{th} values result in activation counts less than N_{RH} for all $|R_1|$ values. From Fig. 3b, we observe that PRAC-N provides security at N_{RH}

values as low as 20 (because a row can receive 19 activations as annotated) when configured to 1) trigger a back-off as frequently as possible ($N_{BO} = 1$) and 2) issue four RFMs in the recovery period (i.e., PRAC-4). For the remaining sections, we configure PRFM and PRAC using these secure thresholds.⁶ We also assume that PRAC *borrow*s time from periodic refreshes to transparently refresh the potential victims of one aggressor row every other periodic refresh command (an operation we call *borrowed refresh*, as shown to be possible in modern DRAM chips [68]), thereby reducing the number of back-offs needed. We do *not* consider periodic refreshes in our security analysis because the memory controller can potentially delay a periodic refresh up to 4 times [144]. These delays result in a maximum time between two consecutive *REF* commands of $5 * t_{REFI}$ (i.e., 19500 ns or 414 row activations for a single DDR5 bank with $t_{RC} = 47$ ns). This large window where the DRAM cells *cannot* be protected with a periodic refresh significantly reduces the security of mechanisms that rely on borrowed refreshes.

6. Overhead Analysis of PRAC

We evaluate PRAC’s performance overheads for existing and future DRAM chips, by sweeping N_{RH} from 1K down to 20 (lowest secure N_{RH} value for PRAC). To evaluate performance, we conduct cycle-level simulations using Ramulator 2.0 [151, 152] (which builds on the original Ramulator [187, 188]). We extend Ramulator 2.0 with the implementations of PRAC, RFM, and the back-off signal. We evaluate system performance using the weighted speedup metric [189, 190].

Table 2 shows our system configuration. We assume a realistic quad-core system, connected to a dual-rank memory with eight bank groups, each containing four banks (64 banks total). The memory controller employs the FR-FCFS memory scheduler [191, 192] with a Cap on Column-Over-Row Reordering (FR-FCFS+Cap) [193] of four. We extend the memory controller to delay requests that *cannot* be served within t_{ABOACT} .

Table 2: Simulated System Configuration

Processor	4.2 GHz, 4-core, 4-wide issue, 128-entry instr. window
Last-Level Cache	64-byte cache line, 8-way set-associative, 8 MB
Memory Controller	64-entry read/write request queues; Scheduling policy: FR-FCFS+Cap of 4 [193]; Address mapping: MOP [194]
Main Memory	DDR5 DRAM [152], 1 channel, 2 ranks, 8 bank groups, 4 banks/bank group, 64K rows/bank

Workloads. We evaluate applications from five benchmark suites: SPEC CPU2006 [195], SPEC CPU2017 [196], TPC [197], MediaBench [198], and YCSB [199]. We group all applications into three memory-intensity groups based on their row buffer misses per kilo instructions (RBMPKIs), similar to prior works [32, 33]. These groups are High (H), Medium (M), and Low (L) for the lowest MPKI values of 10, 2, and 0, respectively. Then, we create 60 workload mixes with 10 of each HHHH, MMMM, LLLL, HHMM, MLLL, and LLHH combination types. We simulate each workload until all cores execute 100M instructions each.

⁶In this study, we assume that we can accurately determine N_{RH} . However, that is a difficult problem, as determining N_{RH} for every row has many challenges and a time-consuming process [1, 16, 135, 136, 143, 183–186].

6.1. Performance Evaluation

Fig. 4 presents the performance overheads of the evaluated read disturbance mitigation mechanisms as N_{RH} decreases. Axes respectively show the N_{RH} values (x axis) and system performance (y axis) in terms of weighted speedup [189, 190] normalized to a baseline with *no* read disturbance mitigation (higher y value is better). Different bars identify different read disturbance mitigation mechanisms and the red edge color indicates unsafe (i.e., read disturbance vulnerable) configurations. We make six observations from Fig. 4.

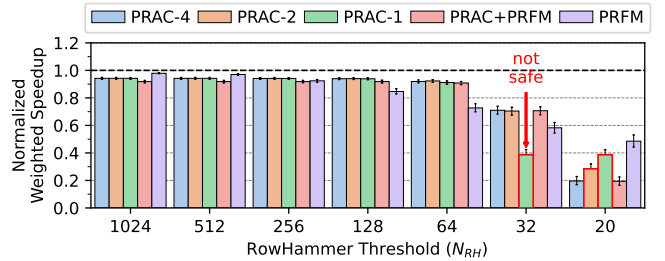


Figure 4: Performance impact of evaluated PRAC and RFM configurations on 60 benign four-core workloads

- Reducing N_{RH} increases performance overheads.** As N_{RH} decreases, performance overheads of all studied mitigation configurations increase, as expected, due to the more frequent mitigating actions (i.e., preventive refreshes) performed.
- PRAC has non-negligible performance overheads.** At $N_{RH} = 1K$, PRAC-4 incurs an average (maximum) system performance overhead of 5.8% (8.9%) across all workloads. We attribute PRAC’s non-negligible overhead at relatively high N_{RH} values to PRAC’s increased DRAM timing parameters [144] (§3) as PRAC-4 sends only 6 back-offs (1.9×10^{-8} back-offs per million cycles) on average across all workloads.
- PRAC overheads slightly increase until $N_{RH} = 64$.** When N_{RH} decreases from 1K to 64, PRAC-4’s system performance overheads slightly increase (i.e., $\approx 2\%$). We attribute the steady system performance as N_{RH} decreases to PRAC accurately tracking aggressor row activations and refreshing rows by *borrowing* time from periodic refreshes.
- PRAC becomes prohibitively expensive at $N_{RH} \leq 64$.** Between N_{RH} values of 64 and 20, PRAC-4’s average (maximum) system performance overheads across all workloads significantly increase from 8.1% (11.8%) to 78.5% (90.7%). We attribute the significant increase in system performance overhead to PRAC performing more frequent preventive refreshes. For example, with PRAC-4 at N_{RH} values of 64 and 20, the four-core benign workload of 523.xalancbmk, 435.gromacs, 459.GemsFDTD, and 434.zeusmp trigger 13.4 and 125.5 back-offs per million cycles, resulting in 15.5% and 87.4% system performance overhead, respectively.
- PRFM performs poorly.** When N_{RH} decreases from 1K to 20, the average (maximum) system performance overhead of PRFM increases from 2.1% (3.7%) to 51.8% (68.7%). We attribute this significant overhead increase to PRFM’s configuration against the wave attack drastically increasing the frequency of preventive refreshes as N_{RH} decreases, similar to PRAC.

6. PRAC+PRFM performs poorly. Pairing PRAC-4 with PRFM increases PRAC’s system performance overhead by an average (maximum) of 21.0% (27.9%) across all N_{RH} values. This is because 1) PRAC’s secure configurations (§5) already preventively refresh all rows before they reach a critical level and 2) pairing PRAC with PRFM causes performance degradation due to unnecessary preventive refreshes.

We conclude that 1) PRAC’s increased DRAM timing parameters incur significant overheads even under infrequent preventive refreshes for modern DRAM chips (i.e., $N_{RH} = 1K$), 2) PRAC’s system performance overheads slightly increase as N_{RH} decreases until 32, where PRAC starts performing significantly worse, 3) PRFM incurs significant system performance loss with decreasing N_{RH} , and 4) pairing PRAC with PRFM provides no system performance advantage.

6.2. PRAC’s Two Major Outstanding Problems

We identify two major outstanding problems with PRAC. First, PRAC counters are incremented while a DRAM row is closed. Doing so increases some timing parameters and degrades system performance. Second, PRAC allows a fixed number of preventive refreshes with each back-off and forces the memory controller to send the same number of activations as refreshed rows before new preventive refreshes can be requested. The possible number of row activations exceeds the number of preventive refreshes performed with PRAC’s preventive actions. Thus, PRAC is vulnerable to the wave attack [20, 147], which significantly reduces the necessary thresholds to mitigate read disturbance and makes mounting memory performance attacks [193] easier (§11).

7. Chronus: Alleviating Counter Access Latencies and Back-Off Delays

We propose Chronus, a new mechanism that addresses PRAC’s two major weaknesses. Chronus implements two key components to address these weaknesses: *Concurrent Counter Update* (CCU) and *Chronus Back-Off*. First, CCU updates row activation counters concurrently while serving accesses. Chronus achieves this by physically separating counters from the data stored in the DRAM array. As such, Chronus prevents the increase in DRAM timing parameters due to PRAC. Second, Chronus Back-Off extends PRAC’s back-off policy such that Chronus performs as many preventive refreshes as needed when a back-off is triggered as opposed to PRAC’s policy of *only* allowing a fixed number of preventive refreshes and enforcing a delay between consecutive back-offs to serve memory accesses. By doing so, Chronus prevents an attacker from maliciously using the back-off delay for a wave attack.

7.1. CCU: Concurrent Counter Update

The latest JEDEC DDR5 DRAM specification (as of April 2024 [144]) allows manufacturers to extend DRAM rows with counter bits. These row activation counters are incremented while the row is being closed, which increases critical DRAM timing parameters (§3) and degrades system performance even at relatively high read disturbance thresholds, e.g., $N_{RH} = 1K$, as

we show in §6. These performance overheads can be eliminated by updating counters *concurrently while serving accesses*, i.e., Concurrent Counter Update (CCU). To achieve this, we propose physically separating counters from data by leveraging subarray-level parallelism [8, 157, 200, 201].

High Level Explanation. Fig. 5 depicts a high-level overview of Chronus’ separate counters. We propose leveraging subarray-level parallelism by storing row activation counters of a DRAM bank in a sufficiently small (e.g., 64-row) additional subarray, which we call the *counter subarray* ❶, within each bank. The counter subarray 1) stores the row activation counts of all data rows in the bank, 2) implements custom circuitry to update ❷ (read – increment by 1 – write back) an activation count when a row is activated, and 3) employs a mechanism to prevent bitflips within the counter subarray ❸. As the counter subarray can be accessed concurrently with *regular subarrays* that store data [8, 157, 200–202], the latency of reading, updating, and writing a counter can be hidden by the latency of opening, accessing, and closing the corresponding row.⁷

Storing the Counters ❶. Chronus leverages the high density of the DRAM array by storing the activation counters in a set of DRAM rows, located in the counter subarray. Assuming a realistic implementation, where 1) each row has an 8-bit row activation count,⁸ 2) a DRAM bank contains 128K DRAM rows [144], and 3) each DRAM row contains 16Kbit in a DRAM chip [144], Chronus maintains 128KB (128K rows \times 8-bits) of activation count metadata for a DRAM bank of 256MB (128K rows \times 16Kbit), which fits into 64 DRAM rows (128KB / 16Kbit). As such, the counter subarray incurs only a 0.05% of capacity overhead.

Updating the Counters ❷. When a DRAM row is activated, Chronus updates the corresponding activation counter in five steps. First, Chronus activates the row that contains the corresponding activation count in the counter subarray. Second, Chronus reads the column that contains the corresponding activation count. Third, Chronus reads the activation count by parsing the corresponding bits in the read column. Fourth, Chronus updates the activation count. Fifth, Chronus writes the updated counter back. To read/write the counter, Chronus parses three sets of bits from the externally provided row address and identifies the row, column, and byte addresses used in the counter subarray. To achieve low hardware complexity, Chronus uses custom circuitry to decrement the counter for a row by one (we call this circuit *the decrementer circuit*) when the row is activated and triggers a back-off when the counter reaches zero (e.g., every 256 activations). For N_{RH} values smaller than 256, Chronus compares the counter against $256 - N_{RH}$ and triggers a back-off accordingly.

We implement the decrementer circuit using NAND, NOR, NOT, and MUX gates (gates that are already implemented in

⁷We propose using subarray-level parallelism [157] only between the counter subarray and regular subarrays. Chronus can also be combined with exploiting subarray-level parallelism between regular subarrays [157]. We leave the exploration of the benefits and challenges of such design to future work.

⁸Chronus’s performance and energy overheads are reasonably low (<0.1%) for an N_{RH} of 256 (§10). Therefore, we assume a counter width of 8 bits.

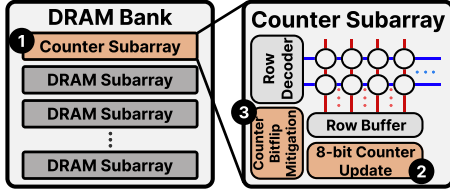


Figure 5: Overview of Chronus’ Concurrent Counter Update technique

the local sense amplifiers). Our design consists of 21 gates and can be implemented with 96 transistors. We evaluate the critical path delay of the decremter circuit to be 0.627 ns,⁹ which is significantly smaller than the row cycle latency (t_{RC}) of 47 ns and hence can be completed concurrently with an access to another subarray. Appendix A provides a detailed implementation of the decremter circuit.

Avoiding Bitflips in the Counter Subarray ③. The counter subarray consists of DRAM cells and thus it is also vulnerable to read disturbance bitflips. To avoid bitflips in the counter subarray, we recommend implementing one of three effective countermeasures: 1) tracking the activation counts of rows in the counter subarray in a separate SRAM array and refreshing them when necessary, similar to the Silver Bullet technique [20, 147], 2) refreshing potential victim rows in the counter subarray frequently in parallel to accessing other rows by latching the fetched row in a redundant array of sense amplifiers, similar to REGA [175], and 3) allocating guard rows in between consecutive rows in the counter subarray, similar to GuardION [45] and ZebRAM [94]. Although these can be costly solutions for protecting all rows, their costs can be reasonable when limited to the counter subarray (equivalent to protecting only 0.05% of a DRAM bank). Our CACTI [206] and mathematical evaluations show that applying any of these solutions incur near-zero (<0.1%) area overhead per DRAM bank.

Resetting the Counters. As DRAM cells are periodically refreshed to retain their data, DRAM read disturbance mechanisms periodically reset activation counters to reduce the number of preventive actions taken [4, 17, 24, 32, 33]. Doing so also prevents an adversarial access pattern that can hog a significant amount of DRAM bandwidth availability due to preventive actions. This adversarial pattern 1) hammers many rows close to the preventive action threshold and 2) triggers preventive

actions on each row quickly.¹⁰ To reduce the number of preventive actions (i.e., back-off) and to mitigate the adversarial access pattern, Chronus borrows time from periodic refreshes (similarly to PRAC, as we describe in §5). As such, Chronus periodically refreshes the victims of a *recently accessed row with a relatively high activation count*, thereby 1) resetting the counter of the row before it is activated enough times to trigger a back-off and 2) preventing the build-up of an adversarial access pattern that could hog DRAM bandwidth availability.

DRAM Energy Overhead of the Counter Subarray. A row activation in the counter subarray (which is concurrent with an activation of a row in a regular subarray) does *not* significantly increase DRAM power consumption, as shown by two independent prior studies [181, 202]. First, real DRAM chip measurements with multiple row activations [202] show that additional row activations introduce marginal additional power consumption, e.g., simultaneously activating 32 rows consumes 21.19% less power than a periodic refresh operation. Second, a separate prior work [181] shows that power consumption largely comes from driving the peripheral circuitry instead of asserting wordlines. For our evaluations, we conduct SPICE [208] simulations using prior state-of-the-art open-source DRAM subarray models [37] to estimate Chronus’ power and energy overheads. Our SPICE simulations show that the row activation in the counter subarray and the counter update increase the DRAM energy consumption of a DRAM row access (i.e., opening and closing a row) by 19.07%.

7.2. Chronus Back-Off

The wave attack is only possible if an attacker can perform row activations more quickly than the read disturbance mitigation mechanism refreshes victims. Fig. 6 visualizes the wave attack buildup for four classes of mitigation mechanisms: (a) Memory Controller Based [1, 3–24, 38, 40–81], (b) Refresh Management [144], (c) PRAC Back-Off [144], and (d) Chronus Back-Off (this work).

The memory controller based mechanisms control the flow of traffic to DRAM. Therefore, these mechanisms can stop serving DRAM accesses and freely refresh all potential victims of aggressor rows that reach a critical activation count (e.g., 32 in Fig. 6). Refresh Management, as described in the JEDEC standard [144], requires RFM commands to be issued periodically based on the number of activations to a bank. Therefore, the activations between periodic preventive refreshes enable a wave

⁹We use the Synopsys Design Compiler [203] with a Global Foundries 22nm technology [204], configured to take into account the performance degradation of implementing logic using the DRAM process. We set the output load of the decremter circuit to be 1000fF and apply a latency penalty factor of 22.91% used in prior work [205].

¹⁰An attacker can also hog a significant amount of DRAM bandwidth availability with different adversarial access patterns at future N_{RH} values, as shown by prior work [207]. We perform a similar study by analyzing Chronus and PRAC’s vulnerability to memory performance attacks [193] in §11.

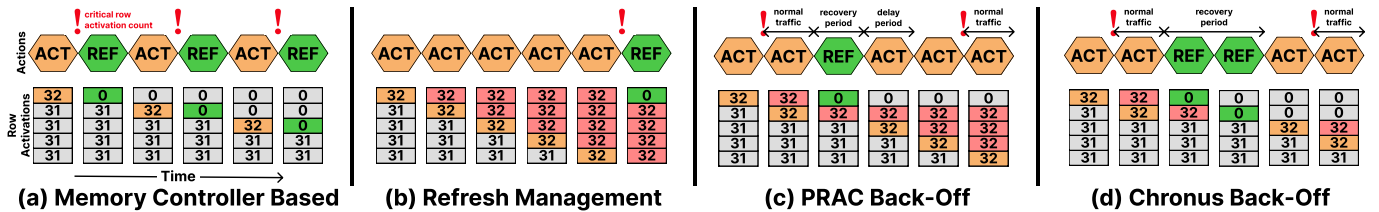


Figure 6: Wave attack visualization for four different classes of read disturbance mitigation mechanisms

attack. PRAC Back-Off suffers from three limitations that both reduce performance and enable a wave attack: *L1*) The memory controller *can* issue activations (with a maximum number of $180 \text{ ns}/t_{RC}$ after a back-off is triggered (during the window of normal traffic), *L2*) the memory controller inefficiently sends a fixed number of preventive refresh commands (N_{Ref}) with each back-off (regardless of the number of preventive refreshes needed to refresh all potential victims), and *L3*) the DRAM module *cannot* trigger another back-off (delay period) until the DRAM module receives a certain number of activations (N_{Delay}). In contrast, Chronus Back-Off securely *prevents* a wave attack (and performance loss due to unnecessary preventive refreshes) by solving two key weaknesses (*L2* and *L3*)¹¹ of PRAC Back-Off. First, Chronus keeps the back-off signal asserted until the DRAM module refreshes the last aggressor row with an activation count that exceeds N_{BO} . While the back-off signal is asserted, the memory controller continues to send preventive refreshes. Second, Chronus does *not* enforce a delay period. Doing so prevents unnecessary refreshes by allowing Chronus to dynamically adjust the number of preventive refreshes.

Challenges of Enabling Chronus Back-Off. We discuss two design considerations to enable Chronus Back-Off: 1) latency of the back-off signal and 2) re-asserting the back-off signal without a delay period. First, the latency of the back-off signal is low enough to provide dynamic control over the number of RFM commands because an RFM command has a relatively high duration (e.g., 350 ns [144]). This high duration is enough for the memory controller to acknowledge the de-asserted back-off signal and stop sending RFM commands; The JEDEC DDR5 standard [144] already utilizes the pin used by back-off signals (i.e., `alert_n` pin) at a lower latency in two places: 1) *Write CRC Error Handling* [144] requires `alert_n` to be asserted for 12 to 20 command clock cycles with a potential delay of 3 ns to 13 ns and 2) *PRAC Back-Off* [144] requires the memory controller to acknowledge `alert_n` with a latency of 180 ns (i.e., duration of normal traffic). Second, *PRAC Back-Off* already *allows* the `alert_n` to be asserted during the delay period due to other causes (e.g., Write DQ CRC errors [144]). We conclude that there are *no* fundamental limitations in the JEDEC DDR5 standard [144] against enabling Chronus Back-Offs.

8. Security Analysis of Chronus

We analyze the security of Chronus against read disturbance bitflips. We base our analysis on Chronus’s three key properties: *P1*) Chronus accurately tracks the activation count of all rows (as it employs per row activation counters); *P2*) Chronus can trigger a back-off at any time (as it does *not* enforce a delay period); and *P3*) Chronus back-offs remain in effect until all rows that reach the back-off threshold have been refreshed.

Let $A(i)$ denote the activation count of row i and N_{BO} denote

¹¹We do *not* propose reducing or removing the window of normal traffic (*L1*) because such a change requires 1) the `alert_n` to be a fast signal and 2) the memory controller to react to a back-off more quickly, thereby potentially increasing memory scheduling complexity. We leave a rigorous analysis of using a more intelligent DRAM interface and protocol (such as [150]) together with Chronus to future work.

the back-off threshold. We assume that a read disturbance bitflip is only possible if a row can be activated at least N_{RH} times before its victims are preventively refreshed. Therefore, a system is secure if and only if $A(i) < N_{RH}$ holds for all rows i at all times. We prove that Chronus is secure against read disturbance bitflips by investigating the system state in four phases: 1) before a back-off is triggered, 2) during the window of normal traffic, 3) during the recovery period, and 4) after the recovery period.

First, before a back-off is triggered, the maximum number of activations to a single row can be at most $N_{BO} - 1$ (following from property *P1* and property *P2*). Second, during the window of normal traffic (after a back-off is triggered), a single row can be activated at most $A_{normal} = 180 \text{ ns}/t_{RC}$ times before the first preventive refresh is issued. Therefore, the total number of activations to a row i before the memory controller issues the first preventive refresh is $A(i) = N_{BO} + A_{normal}$ (because N_{BO} th activation triggers the back-off). Third, during the recovery period, Chronus preventively refreshes the potential victims and resets the activation counts of all rows i where $A(i) \geq N_{BO}$ (following from property *P1* and property *P3*). Fourth, after the recovery period, a row has at most $N_{BO} - 1$ activations (which is the same as step one).

These four phases show that Chronus performs preventive refreshes in a way that $A(i) \leq N_{BO} + A_{normal}$ for all i at all times. Therefore, Chronus is secure against read disturbance bitflips in configurations where $N_{BO} < N_{RH} - A_{normal}$.

Determining a Secure Aggressor Tracking Table Size. An attacker can try to overwhelm the *Aggressor Tracking Table* (ATT, see §3) by forcing many rows to reach N_{BO} activations. Our proof shows that an attacker can perform at most A_{normal} additional activations after triggering a back-off. The attacker can maximize the number of rows that require a refresh in three steps. First, the attacker activates $A_{normal} + 1$ rows $N_{BO} - 1$ times each *without* triggering a back-off. Second, the attacker activates one of the rows for the N_{BO} th time, which triggers a back-off. Third, the attacker activates the other A_{normal} rows that did *not* trigger the back-off for the N_{BO} th time during the window of normal traffic. By doing so, an attacker can force at most $A_{normal} + 1$ rows to reach N_{BO} activations. Therefore, ATT should be able to hold at least $A_{normal} + 1$ entries (e.g., $\lfloor 180 \text{ ns}/t_{RC} \rfloor + 1 = 4$ entries for a t_{RC} of 47 ns).

9. Experimental Methodology

We evaluate Chronus’s overheads on performance and DRAM energy consumption for existing and future DRAM chips, by sweeping N_{RH} from 1K down to 20. We consider two Chronus variants to separately assess the effects of Concurrent Counter Update (CCU) and Chronus Back-Off: 1) *Chronus*, our complete proposal that implements both CCU and Chronus Back-Off and 2) Chronus with PRAC Back-Off (*Chronus-PB*), which implements only CCU and, like PRAC, *always* sends four preventive refreshes *with* a delay period (i.e., PRAC-4 with CCU). **Comparison Points.** We compare Chronus to PRAC [144], PRFM [144], and three state-of-the-art read disturbance mitigation mechanisms: 1) *Graphene* [4], a deterministic mech-

anism that uses the Misra-Gries frequent item counting algorithm [209] and maintains frequently accessed row counters completely within the memory controller; 2) *PARA* [1], a probabilistic memory-controller-based mechanism that does *not* maintain any counters; and 3) *Hydra* [24], a deterministic mechanism that maintains counters in the DRAM chip and caches them in the memory controller. Appendix C compares Chronus to ABACuS, a storage-optimized deterministic mechanism that maintains counters in the memory controller.¹² To evaluate performance and DRAM energy consumption, we conduct cycle-level simulations using Ramulator 2.0 [151, 152], integrated with DRAMPower [210]. We extend Ramulator 2.0 [151, 152] with the implementations of Chronus and open source all of our code and scripts [154]. We use the same system configuration and workloads in §6.

10. Experimental Evaluation

Single-core Performance. Fig. 7 presents the performance overheads of the evaluated read disturbance mitigation mechanisms for different single-core applications at N_{RH} values of 1K (top) and 32 (bottom). Axes respectively show the single-core applications (x axis) and system performance (y axis) in terms of weighted speedup normalized to a baseline with *no* read disturbance mitigation. Different bars identify different read disturbance mitigation mechanisms. *geomean* depicts the geometric mean of each mechanism across 57 single-core applications and error bars show the standard error of the mean [211].

We make two observations from Fig. 7. First, at $N_{RH} = 1K$, Chronus incurs the lowest system performance overhead ($<0.1\%$ on average) across all evaluated mitigation mechanisms. We attribute the low system performance overhead of Chronus at relatively high N_{RH} values (i.e., $N_{RH} \geq 1K$) to the CCU mechanism of Chronus because Chronus-PB (which implements CCU but *not* Chronus Back-Off) performs similarly well at these thresholds. Second, Chronus outperforms all mitigation mechanisms even at very low N_{RH} values. At $N_{RH} = 32$, Chronus induces *only* 6.8% average system performance overhead. In contrast, Graphene, Hydra, and PRAC-4 induce 28.1%, 30.6%, and 42.5% average system performance overhead, respectively. We attribute the low system performance overhead of Chronus

¹²We evaluate ABACuS separately because ABACuS performs best with ABACuS’s own DRAM address mapping configuration (as described in [33]).

at relatively low N_{RH} values (i.e., $N_{RH} \leq 32$) to securely preventing a wave attack and thereby having a less aggressive back-off threshold because Chronus-PB and PRAC, mechanisms that are vulnerable to a wave attack due to using PRAC Back-Off, both induce high system performance overheads (respectively 32.2% and 42.5%) for these same thresholds.

We conclude that 1) Chronus incurs the lowest system performance overhead to single-core applications at N_{RH} values similar to current DRAM chips (e.g., $N_{RH} = 1K$) and 2) Chronus is the best performing mechanism with $<6.8\%$ system performance overhead at future N_{RH} values (e.g., $N_{RH} < 64$).

Multi-core System Performance. Fig. 8 presents the performance overheads of the evaluated read disturbance mitigation mechanisms across 60 benign four-core workloads for N_{RH} values from 1K to 20. x and y axes respectively show the N_{RH} values and system performance in terms of weighted speedup normalized to a baseline with *no* read disturbance mitigation (higher y value is better). Each colored bar depicts the mean system performance of a mechanism across 60 four-core workloads and error bars show the standard error of the mean across 60 four-core workloads.

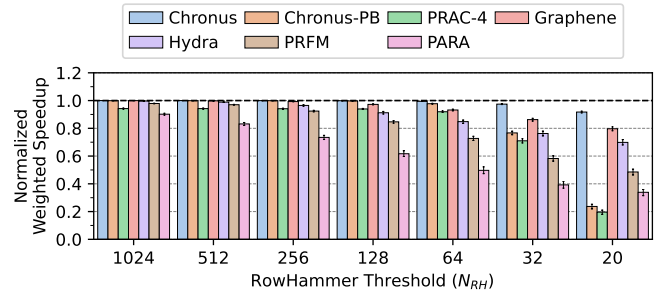


Figure 8: Performance impact of evaluated read disturbance mitigation mechanisms on 60 benign four-core workloads

We make four observations from Fig. 8. First, across all evaluated N_{RH} values, Chronus outperforms all evaluated read disturbance mitigation mechanisms. Second, across all evaluated mechanisms, Chronus’s system performance scales the best as the concurrently running application count in a workload increases. For example, as the concurrently running application count increases from one (57 single-core workloads total in Fig. 7) to four (60 four-core workloads total in Fig. 8) at $N_{RH} = 32$, Chronus’s average system performance improves re-

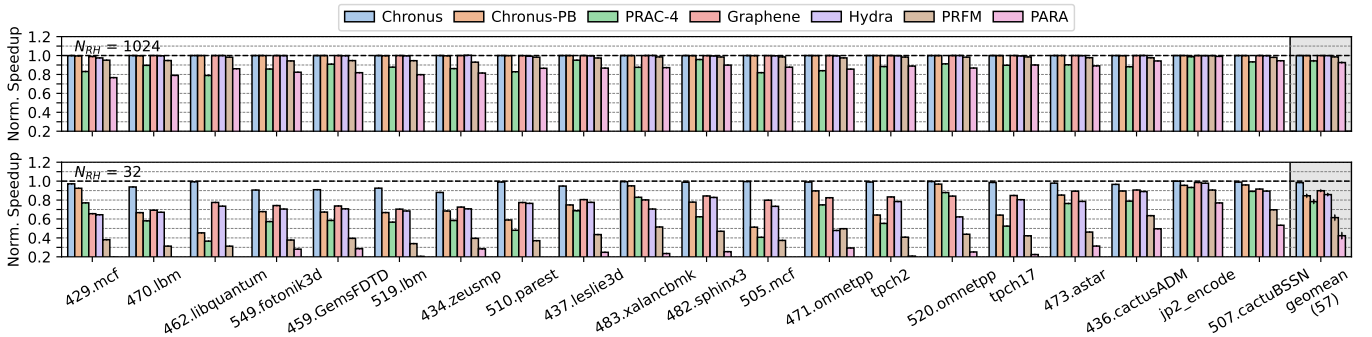


Figure 7: Performance impact of evaluated read disturbance mitigation mechanisms on benign single-core workloads

spectively over PRAC-4 by 18.0%, Graphene by 14.8%, Hydra by 5.0%, and PARA by 64.4%. Third, as N_{RH} decreases, the system performance overhead of all evaluated mitigation mechanisms increases. Fourth, PRAC-4 underperforms against all evaluated mitigation mechanisms at $N_{RH} = 20$. This is because PRAC-4 inefficiently performs 4 preventive refreshes with each back-off and requires conservative configuration against a potential wave attack. In contrast, Chronus’s performance does *not* get drastically (i.e., $\geq 10\%$ overhead) exacerbated at $N_{RH} = 20$ for two reasons: Chronus 1) dynamically adjusts the number of preventive refreshes as necessary and 2) can be less aggressively configured due to its mechanism securely preventing a potential wave attack.

We conclude that 1) Chronus incurs low system performance overhead on evaluated multi-core workloads at N_{RH} values similar to current DRAM chips (e.g., $N_{RH} = 1K$) and 2) Chronus scales the best to future N_{RH} values (e.g., $N_{RH} < 64$) with $< 8.3\%$ system performance overhead.

Sensitivity to Workload Memory Intensity. We further study the system performance overhead of each mechanism at different memory intensity levels. Fig. 9 presents the performance overheads of the evaluated read disturbance mitigation mechanisms for four-core workload types of varying intensities at $N_{RH} = 32$. Axes respectively show the workload types (x axis) and system performance (y axis) in terms of weighted speedup normalized to a baseline with *no* read disturbance mitigation (higher y value is better). Each letter in the workload type identifies the memory intensity of an application as High (H), Medium (M), or Low (L). In each workload type, colored bars show the mean system performance of a mechanism across 10 workloads and error bars show the standard error of the mean across 10 workloads. *geomean* depicts the geometric mean of each mechanism across 60 four-core workloads.

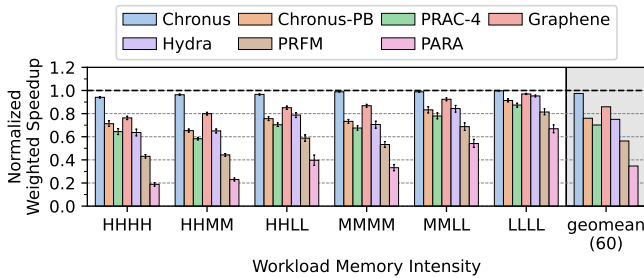


Figure 9: Performance impact of evaluated read disturbance mitigation mechanisms on six workload types of varying memory intensities

We make two observations from Fig. 9. First, Chronus outperforms all evaluated mitigation mechanisms across all workload intensity types. Second, the system performance overhead of evaluated mitigation mechanisms increases with the memory intensity of the workloads. We conclude that Chronus’s system performance stays the best with varying memory intensity.

DRAM Energy. We study the DRAM energy overheads of read disturbance mechanisms. Fig. 10 presents the energy consumption of the evaluated read disturbance mitigation mechanisms (y axis) normalized to a baseline with *no* read disturbance miti-

gation mechanism as N_{RH} (x axis) decreases. Each colored bar depicts the mean energy consumption of a mechanism across 60 four-core workloads and error bars show the standard error of the mean across 60 four-core workloads.

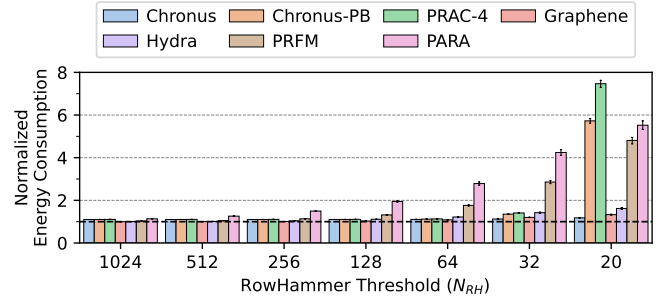


Figure 10: Energy impact of evaluated read disturbance mitigation mechanisms on 60 benign four-core workloads

We make seven observations from Fig. 10. First, as N_{RH} decreases, the energy overheads of all evaluated mitigation mechanisms increases. Second, at $N_{RH} = 1K$, Chronus increases the average (maximum) energy consumption by 10.3% (10.7%) over a baseline with *no* read disturbance mechanism. At this threshold, Chronus has 3.5% lower energy overhead than PRAC-4. This is because Chronus’s CCU mechanism introduces less energy overhead than PRAC’s energy overheads, which are high due to higher DRAM timing parameters and consequently slower execution. Third, when N_{RH} decreases from 1K to 20, Chronus’s average (maximum) energy overhead increases from 10.3% (10.7%) to 17.9% (20.7%). Fourth, Chronus leads to lower energy consumption than all evaluated mitigation mechanisms at $N_{RH} \leq 64$. Fifth, when N_{RH} decreases from 1K to 20, PRFM’s average energy overhead increases from $< 1.1x$ to $4.8x$. Sixth, when N_{RH} decreases from 1K to 20, PRAC-4’s average energy overhead significantly increases from $1.1x$ to $6.6x$. We attribute the high increases in energy consumption overheads of PRFM and PRAC-4 as N_{RH} decreases to 1) their conservative preventive refresh thresholds against a potential wave attack and 2) benign applications triggering many preventive refreshes. Seventh, as N_{RH} decreases from 1K to 20, average energy overheads of Graphene and Hydra increase greatly, from $< 0.1\%$ and 0.3% to 33.0% and 62.0% , respectively.

We conclude that 1) Chronus consumes lower DRAM energy compared to PRAC at N_{RH} values similar to current DRAM chips (e.g., $N_{RH} = 1K$) and 2) Chronus is the lowest energy-overhead solution at future N_{RH} values (e.g., $N_{RH} < 64$).

Storage. Fig. 11 shows the storage overhead in MiB (y axis) of the evaluated read disturbance mitigation mechanisms as N_{RH} decreases (x axis). We evaluate the storage usage of Chronus (DRAM), Graphene (CAM), Hydra (DRAM+SRAM), PRAC (DRAM), and PRFM (SRAM) as a function of N_{RH} for a DRAM module with 64 banks and 128K rows per bank.¹³

We make four observations from Fig. 11. First, as N_{RH} decreases from 1K to 20, Chronus’s storage overhead in DRAM

¹³PARA [1] is *stateless* (i.e., does *not* track or store row activation history) and only requires a random number generator. Therefore, we do *not* include PARA in our storage overhead evaluation.

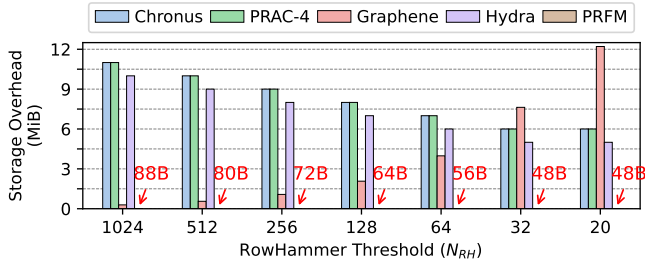


Figure 11: Storage used by Chronus (DRAM), Graphene (CAM), Hydra (DRAM+SRAM), PRAC (DRAM), and PRFM (SRAM) as a function of RowHammer threshold for a DRAM module with 64 banks and 128K rows per bank

is the same as PRAC’s as they both employ a counter per DRAM row. Second, as N_{RH} decreases from 1K to 20, Graphene’s storage overhead in CPU increases significantly (by 50.3x) due to the need to track many more rows. Third, as N_{RH} decreases from 1K to 20, Chronus and Hydra’s storage overheads in DRAM reduce by 45.5% and 50.0%, respectively. We note that while Hydra’s cache structure in CPU does *not* change, the overall cache size reduces with N_{RH} (by 43.9% from 1K to 20) as smaller cache entries are sufficient to track activations. Fourth, PRFM incurs the least storage overhead in the CPU among the evaluated mitigation techniques as it requires only one counter per bank.

We conclude that Chronus, PRAC, PRFM, and Hydra incur low storage overheads and scale well with decreasing N_{RH} values as they either *i*) keep counters in DRAM where a large amount of storage is available at high density or *ii*) require only a small set of counters.

11. Performance Degradation Attack

An attacker can take advantage of Chronus and PRAC to mount memory performance (or denial of memory service) attacks [212] by triggering many back-offs. This section presents 1) the *worst-case* access pattern that causes the maximum theoretical DRAM bandwidth consumption in a Chronus and PRAC-protected system and 2) simulation results.¹⁴

PRAC Theoretical Analysis. We calculate the maximum possible fraction of execution time that preventive actions take in a PRAC-protected system. Triggering a PRAC back-off signal takes $N_{BO} \times t_{RC}$, which causes N_{Ref} RFM commands, blocking the bank for a time window of $N_{Ref} \times t_{RFM}$.¹⁵ Therefore, an attacker can block a DRAM bank for $(N_{Ref} \times t_{RFM}) / (N_{Ref} \times t_{RFM} + N_{BO} \times t_{RC})$ of time. We configure N_{BO} , N_{Ref} , t_{RFM} , and t_{RC} as 1, 4, 350 ns, and 52 ns for $N_{RH} = 20$, based on the DDR5-3200AN speed bin in the JEDEC standard [144]. We observe that an attacker can *theoretically* consume 94% of DRAM throughput by triggering PRAC back-offs.

Chronus Theoretical Analysis. We calculate the maximum possible fraction of execution time that preventive actions take

¹⁴We prove the worst-case property of the adversarial pattern in Appendix D.

¹⁵Attacking rows concurrently in different banks does *not* increase attack efficiency because the memory controller issues all-bank RFM commands (*RFMab*) after a back-off, thereby refreshing the potential victim rows of all concurrent aggressor rows *without* additional overhead.

in a Chronus-protected system. Triggering a Chronus back-off signal takes $N_{BO} \times t_{RC}$, which causes one¹⁶ RFM command, blocking the bank for a time window of t_{RFM} . Therefore, an attacker can block a DRAM bank for $(t_{RFM}) / (t_{RFM} + N_{BO} \times t_{RC})$ of time. We configure N_{BO} , t_{RFM} , and t_{RC} as 16, 350 ns, and 47 ns for $N_{RH} = 20$, based on the DDR5-3200AN speed bin in the JEDEC standard [144]. We observe that an attacker can *theoretically* consume up to 32% of DRAM throughput by triggering Chronus back-offs, which is significantly smaller than PRAC’s *theoretical* overheads (94%).

Simulation. To understand the system performance degradation an attacker could cause by hogging the available DRAM throughput with preventive refreshes, we simulate 60 four-core workload mixes of varying memory intensities where one core maliciously hammers 8 rows in each of 4 banks.¹⁷

Our system performance (weighted speedup [189, 190]) and maximum slowdown of a single application [213] results for N_{RH} values of 128 and 20 show that 1) PRAC-4 reduces system performance on average (maximum) by 15.2% (26.3%) and 84.1% (93.5%) with a maximum slowdown of 63.3% and 97.5%, respectively and 2) Chronus reduces system performance on average (maximum) by 13.3% (24.9%) and 25.9% (39.3%) with a maximum slowdown of 62.3% and 69.9%, respectively. We conclude that Chronus significantly reduces the memory performance attack vulnerability compared to PRAC.

12. Future Research Directions

Although Chronus addresses major weaknesses of PRAC, we believe there is still significant room for improvement in read disturbance solutions (including Chronus and PRAC). In this section, we discuss five directions to improve read disturbance solutions.

A first direction is to determine read disturbance thresholds more accurately. Read disturbance mitigation mechanisms provide security under the assumption that a safe N_{RH} value is known. However, determining a safe N_{RH} value to cover all rows is not easy due to the need to identify the lowest N_{RH} in the presence of N_{RH} variation across data patterns [1, 135, 137, 143, 186], temperature [121, 135], access patterns [120, 136, 143, 214], voltage [137], physical row locations [34, 136], and time [186], as shown by multiple works [1, 16, 121, 135–137, 143, 182, 183, 185, 186, 214]. A second direction to explore is to implement Chronus and PRAC counters more efficiently. Future work can improve the efficiency with *i*) counter update policies against different read disturbance attacks (e.g., RowPress [143])¹⁸ and *ii*) different architectures that improve area and DRAM energy overheads of both Chronus and PRAC. A third direction is to leverage the significant variation in read disturbance vulnerability across rows

¹⁶An attacker should *not* trigger more than one RFM command per back-off as it takes $N_{BO} \times t_{RC}$ per additional RFM command (time to increase another rows activation count), significantly decreasing attack efficiency.

¹⁷We experimentally found these values to yield the highest performance overhead for Chronus and PRAC in our system configuration.

¹⁸One way to mitigate RowPress is to configure RowHammer solutions at lower thresholds (e.g., <500) [143]. We already show that Chronus outperforms state-of-the-art RowPress solutions [1, 4, 24, 144] at such low thresholds.

to avoid overprotecting the vast majority of the rows [34, 136]. For example, Svärd [34] enhances existing RowHammer solutions to become spatial RowHammer threshold aware. Chronus could similarly be combined with Svärd to improve system performance by extending the counter subarray to store the necessary meta-data about the read disturbance vulnerability (e.g., very low, low, average, high) of each row. Chronus already has relatively low performance overheads (e.g., <0.1%) *without* spatial variation awareness even at very low RowHammer thresholds (e.g., <100) and we expect Chronus' performance overheads would further reduce with spatial variation awareness. A fourth direction is to defend against malicious attackers that exploit preventive refreshes. Attackers can trigger increasing amounts of preventive refreshes as N_{RH} decreases, allowing a new attack vector to conduct memory performance attacks [212]. Preventing these performance attacks may be possible by accurately detecting and throttling workloads that trigger many preventive refreshes [18, 207]. A fifth direction is to explore a more flexible DRAM interface design and protocol (as in [150]). Improving the flexibility of the interface and intelligently dividing the work between the memory controller and DRAM by separating the responsibility of handling/controlling access operations (e.g., reading and writing data) and maintenance operations (e.g., DRAM refresh and read disturbance mitigation, like Chronus) can significantly improve system performance and energy, as shown by Self-Managing DRAM [150].

13. Related Work

This is the first work that 1) rigorously analyzes the security and performance and 2) solves the major problems of PRAC, a key feature introduced in the latest JEDEC DDR5 DRAM specification [144] to prevent read disturbance bitflips [1, 143]. An earlier version of this paper [176] analyzes the security and performance benefits of PRAC, but [176] does *not* propose or evaluate a mechanism that solves PRAC's major weaknesses.

We propose Chronus, which addresses the major weaknesses of PRAC by 1) reducing the latency of its counter maintenance operations and 2) preventing adversarial access patterns. §10 and §11 already qualitatively and quantitatively compare Chronus to PRAC and three prominent read disturbance mitigation mechanisms: Graphene [4], PARA [1], and Hydra [24]. We demonstrate that Chronus outperforms these evaluated mechanisms for modern and future DRAM chips. In this section, we discuss other read disturbance mitigation techniques.

Per-Row Activation Tracking. Per-row activation counters were already discussed close to a decade ago in the original RowHammer paper [1] and other works [42, 47, 59, 147]. Building on these works, our paper implements these counters *without* inducing high performance and hardware complexity overheads to modern and future DRAM chips. Panopticon [36] proposes implementing separate per-row counters in a *counter mat* and using the `alert_n` signal to request time for preventive refreshes. Panopticon does *not* discuss performance, energy, or hardware complexity overhead. On the other hand, Chronus replicates an existing DRAM bank structure (i.e., a subarray) and quantifies the performance, energy, and hardware complexity overheads.

Hydra [24], a memory controller-based mechanism, proposes storing per-row tracking entries in DRAM and caching the entries in the memory controller. Hydra does *not* perfectly track per-row activations and does *not* propose a way to update in-DRAM counters concurrently while serving memory requests. In §10, we show that Chronus greatly outperforms Hydra.

Other On-DRAM-Die Mitigation Techniques. DRAM manufacturers implement read disturbance mitigation techniques, also known as Target Row Refresh (TRR) [49, 68, 148, 156], in commercial DRAM chips. The specific designs of these techniques are not openly disclosed. Recent research shows that custom attacks can bypass these mechanisms [14, 49, 68, 92, 117, 118] and cause read disturbance bitflips.

Hardware-based Mitigation Techniques. Prior works propose hardware-based mitigation techniques [1, 3–39] to prevent read disturbance bitflips. Some of these works [1, 6, 8, 11, 16, 39, 215] propose probabilistic preventive refresh mechanisms to mitigate read disturbance at low area cost. These mechanisms do not provide deterministic read disturbance prevention and thus cause high system performance overhead as N_{RH} decreases (as they need to generate many more preventive refreshes). Three prior works [22, 23, 26] propose machine-learning-based mechanisms. These mechanisms are *not* fully secure because they have increasing bitflip probability with lower read disturbance thresholds [22, 23] or they require error-correction codes to correct a small number of bitflips [26]. Another group of prior works [3–5, 7, 12, 17, 25, 28, 29, 33, 35] propose using the Misra-Gries frequent item counting algorithm [209]. Misra-Gries-based mechanisms use a large number of counters implemented with content-addressable memory for low N_{RH} values [32, 33], thereby inducing high hardware area overheads (as we showed for Graphene [4] in §10). In contrast, Chronus provides *deterministic* security guarantees at low N_{RH} values with *low system performance and hardware overheads*.

Software-based Mitigation Techniques. Several software-based read disturbance mitigation techniques [44, 45, 53, 64, 70, 79, 216] propose to avoid hardware-level modifications. However, these works cannot monitor *all* memory requests and thus, many of them are shown to be defeated by recent attacks [93, 100, 105, 108, 112, 115, 217].

Integrity-based Mitigation Techniques. Another set of mitigation techniques [60, 65, 66, 218–222] implements integrity check mechanisms that identify and correct potential bitflips. However, it is either impossible or too costly to address all read disturbance bitflips with these mechanisms.

14. Conclusion

We presented the first rigorous security, performance, energy, and cost analyses of PRAC and proposed a new mechanism, Chronus, which addresses PRAC's two major weaknesses. Our analyses show that PRAC increases the critical DRAM access latency parameters due to the additional time required to increment activation counters and performs a fixed number of preventive refreshes at a time, making it vulnerable to an adversarial access pattern, known as *the wave attack* or *the*

feinting attack. These two weaknesses of PRAC cause significant performance overheads at current and future DRAM chips. Our mechanism, Chronus, solves PRAC's two major problems by 1) updating row activation counters concurrently while serving accesses by physically separating counters from the data and 2) dynamically controlling the number of preventive refreshes performed. Our evaluation shows that Chronus outperforms PRAC and PRFM, the state-of-the-art industry solutions to read disturbance, and three other state-of-the-art read disturbance mitigation proposals in terms of both system performance and DRAM energy, especially for future DRAM chips with higher read disturbance vulnerability. We believe Chronus provides a robust and efficient solution to read disturbance for current and future DRAM chips at low area, performance, and energy costs. We hope that future research continues to improve read disturbance solutions with new ideas, interfaces, and even more efficient techniques.

Acknowledgments

This paper is a significantly extended version of an earlier work presented at DRAMSec 2024 [176]. This version of the paper is an updated version of our original HPCA 2025 conference publication [223] that fixes a bug reported by [224] regarding PRAC's DRAM timing constraints, as described in Appendix E. We thank the anonymous reviewers of DRAMSec 2024 and HPCA 2025 (both main submission and artifact evaluation) for the encouraging feedback. We thank the SAFARI Research Group members for valuable feedback and the stimulating scientific and intellectual environment. We acknowledge the generous gift funding provided by our industrial partners (especially Google, Huawei, Intel, Microsoft, VMware), which has been instrumental in enabling the research we have been conducting on read disturbance in DRAM since 2011 [225]. This work was also in part supported by a Google Security and Privacy Research Award, the Microsoft Swiss Joint Research Center, and the ETH Future Computing Laboratory (EFCL).

References

- [1] Y. Kim, R. Daly, J. Kim, C. Fallin, J. H. Lee, D. Lee, C. Wilkerson, K. Lai, and O. Mutlu. Flipping Bits in Memory Without Accessing Them: An Experimental Study of DRAM Disturbance Errors. In *ISCA*, 2014.
- [2] Robert H. Dennard. Field-Effect Transistor Memory. U.S. Patent 3,387,286, 1968.
- [3] Anish Saxena, Gururaj Saileshwar, Prashant J. Nair, and Moinuddin Qureshi. AQUA: Scalable Rowhammer Mitigation by Quarantining Aggressor Rows at Runtime. In *MICRO*, 2022.
- [4] Yeonhong Park, Woosuk Kwon, Eojin Lee, Tae Jun Ham, Jung Ho Ahn, and Jae W Lee. Graphene: Strong yet Lightweight Row Hammer Protection. In *MICRO*, 2020.
- [5] Michael Jaemin Kim, Jaehyun Park, Yeonhong Park, Wanju Doh, Namhoon Kim, Tae Jun Ham, Jae W Lee, and Jung Ho Ahn. Mithril: Cooperative Row Hammer Protection on Commodity DRAM Leveraging Managed Refresh. In *HPCA*, 2022.
- [6] Jung Min You and Joon-Sung Yang. MRLoc: Mitigating Row-Hammering Based on Memory Locality. In *DAC*, 2019.
- [7] Ingab Kang, Eojin Lee, and Jung Ho Ahn. CAT-TWO: Counter-Based Adaptive Tree, Time Window Optimized for DRAM Row-Hammer Prevention. *IEEE Access*, 2020.
- [8] A. Giray Yağlıkcı, Ataberk Olgun, Minesh Patel, Haocong Luo, Hasan Hassan, Lois Orosa, Oğuz Ergin, and Onur Mutlu. HiRA: Hidden Row Activation for Reducing Refresh Latency of Off-the-Shelf DRAM Chips. In *MICRO*, 2022.
- [9] Hasan Hassan, Ataberk Olgun, A. Giray Yağlıkcı, Haocong Luo, and Onur Mutlu. A Case for Self-Managing DRAM Chips: Improving Performance, Efficiency, Reliability, and Security via Autonomous in-DRAM Maintenance Operations. arXiv:2207.13358 [cs.AR], 2022.
- [10] Ranyang Zhou, Sepehr Tabrizchi, Arman Roohi, and Shaahin Angizi. LT-PIM: An LUT-Based Processing-in-DRAM Architecture with RowHammer Self-Tracking. *CAL*, 2022.

- [11] Mungyu Son, Hyunsun Park, Junwhan Ahn, and Sungjoo Yoo. Making DRAM Stronger Against Row Hammering. In *DAC*, 2017.
- [12] Gururaj Saileshwar, Bolin Wang, Moinuddin Qureshi, and Prashant J Nair. Randomized Row-Swap: Mitigating Row Hammer by Breaking Spatial Correlation Between Aggressor and Victim Rows. In *ASPLOS*, 2022.
- [13] Seong-Wan Ryu, Kyungkyu Min, Jungho Shin, Heimi Kwon, Donghoon Nam, Taekyung Oh, Tae-Su Jang, Minsoo Yoo, Yongtaik Kim, and Sungjoo Hong. Overcoming the Reliability Limitation in the Ultimately Scaled DRAM using Silicon Migration Technique by Hydrogen Annealing. In *IEDM*, 2017.
- [14] Stefan Saroiu, Alec Wolman, and Lucian Cojocar. The Price of Secrecy: How Hiding Internal DRAM Topologies Hurts Rowhammer Defenses. In *IRPS*, 2022.
- [15] Jin Han, Jungsik Kim, Dafna Beery, K Deniz Bozdog, Peter Cuevas, Amitay Levi, Irwin Tain, Khai Tran, Andrew J Walker, Senthil Vadakupudhu Palayam, et al. Surround Gate Transistor With Epitaxially Grown Si Pillar and Simulation Study on Soft Error and Rowhammer Tolerance for DRAM. *TED*, 2021.
- [16] Stefan Saroiu and Alec Wolman. How to Configure Row-Sampling-Based Rowhammer Defenses. *DRAMSec*, 2022.
- [17] Eojin Lee, Ingab Kang, Sukhan Lee, G Edward Suh, and Jung Ho Ahn. TWiCe: Preventing Row-Hammering by Exploiting Time Window Counters. In *ISCA*, 2019.
- [18] A. Giray Yağlıkcı, Minesh Patel, Jeremie S. Kim, Roknoddin Azizibarzoki, Ataberk Olgun, Lois Orosa, Hasan Hassan, Jisung Park, Konstantinos Kanellopoulos, Taha Shahroodi, Saugata Ghose, and Onur Mutlu. BlockHammer: Preventing RowHammer at Low Cost by Blacklisting Rapidly-Accessed DRAM Rows. In *HPCA*, 2021.
- [19] Zvika Greenfield and Tomer Levy. Throttling Support for Row-Hammer Counters, 2016.
- [20] Fabrice Devaux and Renaud Ayrignac. Method and Circuit for Protecting a DRAM Memory Device from the Row Hammer Effect. U.S. Patent 10,885,966, 2021.
- [21] Gyu-Hyeon Lee, Seongmin Na, Ilkwon Byun, Dongmoon Min, and Jangwoo Kim. CryoGuard: A Near Refresh-Free Robust DRAM Design for Cryogenic Computing. In *ISCA*, 2021.
- [22] Biresh Kumar Joardar, Tyler K Bletsch, and Krishnendu Chakrabarty. Learning to Mitigate RowHammer Attacks. In *DATE*, 2022.
- [23] Biresh Kumar Joardar, Tyler K. Bletsch, and Krishnendu Chakrabarty. Machine Learning-Based Rowhammer Mitigation. *TCAD*, 2022.
- [24] Moinuddin Qureshi, Aditya Rohan, Gururaj Saileshwar, and Prashant J Nair. Hydra: Enabling Low-Overhead Mitigation of Row-Hammer at Ultra-Low Thresholds via Hybrid Tracking. In *ISCA*, 2022.
- [25] S. M. Seyedzadeh, A. K. Jones, and R. Melhem. Mitigating Wordline Crosstalk Using Adaptive Trees of Counters. In *ISCA*, 2018.
- [26] Amir Naseredini, Martin Berger, Matteo Sammartino, and Shale Xiong. ALARM: Active Learning of Rowhammer Mitigations. <https://users.sussex.ac.uk/~mfb21/rh-draft.pdf>, 2022.
- [27] Dae-Hyun Kim, Prashant J Nair, and Moinuddin K Qureshi. Architectural Support for Mitigating Row Hammering in DRAM Memories. *CAL*, 2015.
- [28] Jeonghyun Woo, Gururaj Saileshwar, and Prashant J. Nair. Scalable and Secure Row-Swap: Efficient and Safe Row Hammer Mitigation in Memory Systems. arXiv:2212.12613 [cs.CR], 2022.
- [29] Seyed Mohammad Seyedzadeh, Alex K. Jones, and Rami Melhem. Counter-Based Tree Structure for Row Hammering Mitigation in DRAM. *CAL*, 2017.
- [30] Chia Yang, Chen Kang Wei, Yu Jing Chang, Tieh Chiang Wu, Hsiu Pin Chen, and Chao Sung Lai. Suppression of RowHammer Effect by Doping Profile Modification in Saddle-Fin Array Devices for Sub-30-nm DRAM Technology. *TDMR*, 2016.
- [31] H. Gomez, A. Amaya, and E. Roa. DRAM Row-Hammer Attack Reduction Using Dummy Cells. In *NORCAS*, 2016.
- [32] F Nisa Bostanci, Ismail Emir Yüksel, Ataberk Olgun, Konstantinos Kanellopoulos, Yahya Can Tuğrul, A Giray Yağlıcı, Mohammad Sadrosadati, and Onur Mutlu. CoMeT: Count-Min-Sketch-Based Row Tracking to Mitigate RowHammer at Low Cost. In *HPCA*, 2024.
- [33] Ataberk Olgun, Yahya Can Tuğrul, Nisa Bostanci, Ismail Emir Yüksel, Haocong Luo, Steve Rhyner, Abdullah Giray Yağlıkcı, Geraldo F Oliveira, and Onur Mutlu. ABA-CuS: All-Bank Activation Counters for Scalable and Low Overhead RowHammer Mitigation. In *USENIX Security*, 2024.
- [34] A. Giray Yağlıkcı, Yahya Can Tuğrul, Geraldo F De Oliveira, Ismail Emir Yüksel, Ataberk Olgun, Haocong Luo, and Onur Mutlu. Spatial Variation-Aware Read Disturbance Defenses: Experimental Analysis of Real DRAM Chips and Implications on Future Solutions. In *HPCA*, 2024.
- [35] Michele Marazzi, Patrick Jattke, Flavien Solt, and Kaveh Razavi. ProTRR: Principled yet Optimal In-DRAM Target Row Refresh. In *S&P*, 2022.
- [36] Tanj Bennett, Stefan Saroiu, Alec Wolman, and Lucian Cojocar. Panopticon: A Complete In-DRAM Rowhammer Mitigation. *DRAMSec*, 2021.
- [37] H. Hassan, M. Patel, J. S. Kim, A. G. Yağlıkcı, N. Vijaykumar, N. Mansouri Ghiasi, S. Ghose, and O. Mutlu. CROW: A Low-Cost Substrate for Improving DRAM Performance, Energy Efficiency, and Reliability. In *ISCA*, 2019.
- [38] Onur Mutlu, Ataberk Olgun, and A. Giray Yağlıkcı. Fundamentally Understanding and Solving RowHammer. In *ASP-DAC*, 2023.
- [39] Yicheng Wang, Yang Liu, Peiyun Wu, and Zhao Zhang. Discreet-PARA: Rowhammer Defense with Low Cost and High Efficiency. In *ICCD*, 2021.
- [40] Samira Mirbagher Ajorpaz, Daniel Moghimi, Jeffrey Neal Collins, Gilles Pokam, Nael Abu-Ghazaleh, and Dean Tullsen. EVAX: Towards a Practical, Pro-Active & Adaptive Architecture for High Performance & Security. In *MICRO*, 2022.
- [41] Kevin Loughlin, Stefan Saroiu, Alec Wolman, Yatin A. Manerkar, and Baris Kasikci. MOESI-Prime: Preventing Coherence-Induced Hammering in Commodity Workloads. In *ISCA*, 2022.

- [42] K.S. Bains and J.B. Halbert. Distributed Row Hammer Tracking. U.S. Patent 9,299,400, April 3 2016.
- [43] Loïc France, Florent Bruguier, Maria Mushtaq, David Novo, and Pascal Benoit. Modeling Rowhammer in the gem5 Simulator. In *CHES*, 2022.
- [44] Zhi Zhang, Yueqiang Cheng, Minghua Wang, Wei He, Wenhao Wang, Surya Nepal, Yansong Gao, Kang Li, Zhe Wang, and Chenggang Wu. SoftTRR: Protect Page Tables against Rowhammer Attacks using Software-Only Target Row Refresh. In *USENIX ATC*, 2022.
- [45] Victor van der Veen, Martina Lindorfer, Yanick Fratantonio, Harikrishnan Padmanabha Pillai, Giovanni Vigna, Christopher Kruegel, Herbert Bos, and Kaveh Razavi. GuardION: Practical Mitigation of DMA-Based Rowhammer Attacks on ARM. In *DIMVA*, 2018.
- [46] Kevin Loughlin, Stefan Saroiu, Alec Wolman, and Baris Kasikci. Stop! Hammer Time: Rethinking Our Approach to Rowhammer Mitigations. In *HotOS*, 2021.
- [47] Dae-Hyun Kim, Prashant J Nair, and Moinuddin K Qureshi. Architectural Support for Mitigating Row Hammering in DRAM Memories. *CAL*, 2014.
- [48] Kuljit Bains, John Halbert, Christopher Mozak, Theodore Schoenborn, and Zvika Greenfield. Row Hammer Refresh Command. US Patent 9,117,544, 2015.
- [49] Pietro Frigo, Emanuele Vannacci, Hasan Hassan, Victor van der Veen, Onur Mutlu, Cristiano Giuffrida, Herbert Bos, and Kaveh Razavi. TRRespass: Exploiting the Many Sides of Target Row Refresh. In *S&P*, 2020.
- [50] Sonia Sharma, Debdeep Sanyal, Arpit Mukhopadhyay, and Ramij Hasan Shaik. A Review on Study of Defects of DRAM-RowHammer and Its Mitigation. *Journal For Basic Sciences*, 2022.
- [51] Barbara Aichinger. DDR Memory Errors Caused by Row Hammer. In *HPEC*, 2015.
- [52] Hewlett-Packard Enterprise. HP Moonshot Component Pack V2015.05.0, 2015.
- [53] Ferdinand Brasser, Lucas Davi, David Gens, Christopher Liebchen, and Ahmad-Reza Sadeghi. Can't Touch This: Software-Only Mitigation Against Rowhammer Attacks Targeting Kernel Memory. In *USENIX Security*, 2017.
- [54] Lenovo Group Ltd. Row Hammer Privilege Escalation. https://support.lenovo.com/us/en/product_security/row_hammer, 2015.
- [55] Apple Inc. About the Security Content of Mac EFI Security Update 2015-001. <https://support.apple.com/en-us/HT204934>. June 2015.
- [56] C Gude Ramarao, K Tejesh Kumar, G Ujjinappa, and B Vasu Deva Naidu. Defending SoCs with FPGAs from Rowhammer Attacks. *Material Science*, 2023.
- [57] Jeonghyun Woo, Gururaj Saileshwar, and Prashant J Nair. Scalable and Secure Row-Swap: Efficient and Safe Row Hammer Mitigation in Memory Systems. In *HPCA*, 2023.
- [58] Andrea Di Dio, Koen Koning, Herbert Bos, and Cristiano Giuffrida. Copy-on-Flip: Hardening ECC Memory Against Rowhammer Attacks. In *NDSS*, 2023.
- [59] Kuljit S Bains and John B Halbert. Row Hammer Monitoring Based on Stored Row Hammer Threshold Value. US Patent 10,083,737, 2016.
- [60] Jonas Juffinger, Lukas Lamster, Andreas Kogler, Maria Eichlseder, Moritz Lipp, and Daniel Gruss. CSI: Rowhammer-Cryptographic Security and Integrity against Rowhammer. In *SP*, 2023.
- [61] Woongrae Kim, Chulmoon Jung, Seongnyuh Yoo, Duckhwa Hong, Jeongjin Hwang, Jungmin Yoon, Ohyoung Choi, Joonwoo Choi, Sanga Hyun, Mankeun Kang, et al. A 1.1V 16Gb DDR5 DRAM with Probabilistic-Aggressor Tracking, Refresh-Management Functionality, Per-Row Hammer Tracking, a Multi-Step Precharge, and Core-Bias Modulation for Security and Reliability Enhancement. In *ISSCC*, 2023.
- [62] SK Gautam, SK Manhas, Arvind Kumar, Mahendra Pakala, and Ellie Yieh. Row Hammering Mitigation Using Metal Nanowire in Saddle Fin DRAM. *IEEE TED*, 2019.
- [63] K. Bains et al. Row Hammer Refresh Command. U.S. Patents: 9,117,544 9,236,110 10,210,925, 2015.
- [64] Shuhei Enomoto, Hiroki Kuzuno, and Hiroshi Yamada. Efficient Protection Mechanism for CPU Cache Flush Instruction Based Attacks. *IEICE Trans. Inf. Syst.*, 2022.
- [65] Ali Fakhrzadehgan, Yale N. Patt, Prashant J. Nair, and Moinuddin K. Qureshi. SafeGuard: Reducing the Security Risk from Row-Hammer via Low-Cost Integrity Protection. In *HPCA*, 2022.
- [66] Evgeny Manzhosov, Adam Hastings, Meghna Pancholi, Ryan Piersma, Mohamed Tarek Ibn Ziad, and Simha Sethumadhavan. Revisiting Residue Codes for Modern Memories. In *MICRO*, 2022.
- [67] Krishnendu Guha and Amlan Chakrabarti. Criticality Based Reliability from Rowhammer Attacks in Multi-User-Multi-FPGA Platform. In *VLSID*, 2022.
- [68] Hasan Hassan, Yahya Can Tugrul, Jeremie S. Kim, Victor van der Veen, Kaveh Razavi, and Onur Mutlu. Uncovering In-DRAM RowHammer Protection Mechanisms: A New Methodology, Custom RowHammer Patterns, and Implications. In *MICRO*, 2021.
- [69] Minbok Wi, Jaehyun Park, Seoyoung Ko, Michael Jaemin Kim, Nam Sung Kim, Eojin Lee, and Jung Ho Ahn. SHADOW: Preventing Row Hammer in DRAM with Intra-Subarray Row Shuffling. In *HPCA*, 2023.
- [70] Radhesh Krishnan Konoth, Marco Oliverio, Andrei Tatar, Dennis Andriess, Herbert Bos, Cristiano Giuffrida, and Kaveh Razavi. ZebRAM: Comprehensive and Compatible Software Protection Against Rowhammer Attacks. In *OSDI*, 2018.
- [71] Saru Vig, Sarani Bhattacharya, Debdeep Mukhopadhyay, and Siew-Kei Lam. Rapid Detection of Rowhammer Attacks Using Dynamic Skewed Hash Tree. In *HASP*, 2018.
- [72] Chihiro Tomita, Makoto Takita, Kazuhide Fukushima, Yuto Nakano, Yoshiaki Shiraishi, and Masakatu Morii. Extracting the Secrets of OpenSSL with RAMBleed. *Sensors*, 2022.
- [73] Ranyang Zhou, Sabbir Ahmed, Adnan Siraj Rakin, and Shaahin Angizi. DNN-Defender: An In-DRAM Deep Neural Network Defense Mechanism for Adversarial Weight Attack. arXiv:2305.08034 [cs.CR], 2023.
- [74] Gorka Irazoqui, Thomas Eisenbarth, and Berk Sunar. MASCAT: Stopping Microarchitectural Attacks Before Execution. *IACR Cryptology*, 2016.
- [75] Kerem Arıkan, Alessandro Palumbo, Luca Cassano, Pedro Reviriego, Salvatore Pontarelli, Giuseppe Bianchi, Oğuz Ergin, and Marco Ottavi. Processor Security: Detecting Microarchitectural Attacks via Count-Min Sketches. *VLSI*, 2022.
- [76] Chia-Ming Yang, Chen-Kang Wei, Hsiu-Pin Chen, Jian-Shing Luo, Yu Jing Chang, Tieh-Chiang Wu, and Chao-Sung Lai. Scanning Spreading Resistance Microscopy for Doping Profile in Saddle-Fin Devices. *TNANO*, 2017.
- [77] Zhenkai Zhang, Zihao Zhan, Daniel Balasubramanian, Bo Li, Peter Volgyesi, and Xenofon Koutsoukos. Leveraging EM Side-Channel Information to Detect Rowhammer Attacks. In *SP*, 2020.
- [78] Anish Saxena, Gururaj Saileshwar, Jonas Juffinger, Andreas Kogler, Daniel Gruss, and Moinuddin Qureshi. PT-Guard: Integrity-Protected Page Tables to Defend Against Breakthrough Rowhammer Attacks. In *DSN*, 2023.
- [79] Zelalem Birhanu Aweke, Salessawi Ferede Yitbarek, Rui Qiao, Reetuparna Das, Matthew Hicks, Yossi Oren, and Todd Austin. ANVIL: Software-Based Protection Against Next-Generation Rowhammer Attacks. In *ASPLOS*, 2016.
- [80] Loïc France, Florent Bruguier, David Novo, Maria Mushtaq, and Pascal Benoit. Reducing the Silicon Area Overhead of Counter-Based Rowhammer Mitigations. In *18th CryptArchi Workshop*, 2022.
- [81] Jin Hyo Park, Su Yeon Kim, Geon Kim, Je Won Park, Sunyong Yoo, Young-Woo Lee, and Myoung Jin Lee. Row Hammer Reduction Using a Buried Insulator in a Buried Channel Array Transistor. *IEEE TED*, 2022.
- [82] Apostolos P Fournaris, Lidia Pocero Fraile, and Odysseas Koufopavlou. Exploiting Hardware Vulnerabilities to Attack Embedded System Devices: A Survey of Potent Microarchitectural Attacks. *Electronics*, 2017.
- [83] Damian Poddebniak, Juraj Somorovsky, Sebastian Schinzel, Manfred Lochter, and Paul Rösler. Attacking Deterministic Signature Schemes Using Fault Attacks. In *EuroS&P*, 2018.
- [84] Andrei Tatar, Radhesh Krishnan Konoth, Elias Athanasopoulos, Cristiano Giuffrida, Herbert Bos, and Kaveh Razavi. Throwhammer: Rowhammer Attacks Over the Network and Defenses. In *USENIX ATC*, 2018.
- [85] Sebastien Carre, Matthieu Desjardins, Adrien Facon, and Sylvain Guilley. OpenSSL Bellcore's Protection Helps Fault Attack. In *DSD*, 2018.
- [86] Alessandro Barengi, Luca Breveglieri, Niccolò Izzo, and Gerardo Pelosi. Software-Only Reverse Engineering of Physical DRAM Mappings for Rowhammer Attacks. In *IVSW*, 2018.
- [87] Zhenkai Zhang, Zihao Zhan, Daniel Balasubramanian, Xenofon Koutsoukos, and Gabor Karsai. Triggering Rowhammer Hardware Faults on ARM: A Revisit. In *ASHES*, 2018.
- [88] Sarani Bhattacharya and Debdeep Mukhopadhyay. Advanced Fault Attacks in Software: Exploiting the Rowhammer Bug. *Fault Tolerant Architectures for Cryptography and Hardware Security*, 2018.
- [89] Mark Seaborn and Thomas Dullien. Exploiting the DRAM Rowhammer Bug to Gain Kernel Privileges. <http://googleprojectzero.blogspot.com.tr/2015/03/exploiting-dram-rowhammer-bug-to-gain.html>, 2015.
- [90] SAFARI Research Group. RowHammer — GitHub Repository. <https://github.com/CMU-SAFARI/rowhammer>.
- [91] Mark Seaborn and Thomas Dullien. Exploiting the DRAM Rowhammer Bug to Gain Kernel Privileges. *Black Hat*, 2015.
- [92] Victor van der Veen, Yanick Fratantonio, Martina Lindorfer, Daniel Gruss, Clémentine Maurice, Giovanni Vigna, Herbert Bos, Kaveh Razavi, and Cristiano Giuffrida. Drammer: Deterministic Rowhammer Attacks on Mobile Platforms. In *CCS*, 2016.
- [93] Daniel Gruss, Clémentine Maurice, and Stefan Mangard. Rowhammer.js: A Remote Software-Induced Fault Attack in Javascript. *DIMVA*, 2016.
- [94] Kaveh Razavi, Ben Gras, Erik Bosman, Bart Preneel, Cristiano Giuffrida, and Herbert Bos. Flip Feng Shui: Hammering a Needle in the Software Stack. In *USENIX Security*, 2016.
- [95] Peter Pessl, Daniel Gruss, Clémentine Maurice, Michael Schwarz, and Stefan Mangard. DRAMA: Exploiting DRAM Addressing for Cross-CPU Attacks. In *USENIX Security*, 2016.
- [96] Yuan Xiao, Xiaokuan Zhang, Yinqian Zhang, and Radu Teodorescu. One Bit Flips, One Cloud Flops: Cross-VM Row Hammer Attacks and Privilege Escalation. In *USENIX Security*, 2016.
- [97] Erik Bosman, Kaveh Razavi, Herbert Bos, and Cristiano Giuffrida. Dedup Est Machina: Memory Deduplication as an Advanced Exploitation Vector. In *S&P*, 2016.
- [98] Sarani Bhattacharya and Debdeep Mukhopadhyay. Curious Case of Rowhammer: Flipping Secret Exponent Bits Using Timing Analysis. In *CHES*, 2016.
- [99] Wayne Burleson, Onur Mutlu, and Mohit Tiwari. Invited: Who is the Major Threat to Tomorrow's Security? You, the Hardware Designer. In *DAC*, 2016.
- [100] Rui Qiao and Mark Seaborn. A New Approach for RowHammer Attacks. In *HOST*, 2016.
- [101] Yeongjin Jang, Jaehyuk Lee, Sangho Lee, and Taesoo Kim. SGX-Bomb: Locking Down the Processor via Rowhammer Attack. In *SOSP*, 2017.
- [102] Misiker Tadesse Aga, Zelalem Birhanu Aweke, and Todd Austin. When Good Protections Go Bad: Exploiting Anti-DoS Measures to Accelerate Rowhammer Attacks. In *HOST*, 2017.
- [103] Onur Mutlu. The RowHammer Problem and Other Issues We May Face as Memory Becomes Denser. In *DATE*, 2017.
- [104] Andrei Tatar, Cristiano Giuffrida, Herbert Bos, and Kaveh Razavi. Defeating

- Software Mitigations Against Rowhammer: A Surgical Precision Hammer. In *RAID*, 2018.
- [105] Daniel Gruss, Moritz Lipp, Michael Schwarz, Daniel Genkin, Jonas Juffinger, Sioli O’Connell, Wolfgang Schoechl, and Yuval Yarom. Another Flip in the Wall of Rowhammer Defenses. In *S&P*, 2018.
- [106] Moritz Lipp, Misiker Tadesse Aga, Michael Schwarz, Daniel Gruss, Clémentine Maurice, Lukas Raab, and Lukas Lamster. Nethammer: Inducing Rowhammer Faults Through Network Requests. *EuroS&PW*, 2020.
- [107] Pietro Frigo, Cristiano Giuffrida, Herbert Bos, and Kaveh Razavi. Grand Pwning Unit: Accelerating Microarchitectural Attacks with the GPU. In *S&P*, 2018.
- [108] Lucian Cojocar, Kaveh Razavi, Cristiano Giuffrida, and Herbert Bos. Exploiting Correcting Codes: On the Effectiveness of ECC Memory Against Rowhammer Attacks. In *S&P*, 2019.
- [109] Sangwoo Ji, Youngjoo Ko, Saeyoung Oh, and Jong Kim. Pinpoint Rowhammer: Suppressing Unwanted Bit Flips on Rowhammer Attacks. In *ASIACCS*, 2019.
- [110] Onur Mutlu and Jeremie S Kim. RowHammer: A Retrospective. *TCAD*, 2019.
- [111] Sanghyun Hong, Pietro Frigo, Yiğitan Kaya, Cristiano Giuffrida, and Tudor Dumitras. Terminal Brain Damage: Exposing the Graceless Degradation in Deep Neural Networks Under Hardware Fault Attacks. In *USENIX Security*, 2019.
- [112] Andrew Kwong, Daniel Genkin, Daniel Gruss, and Yuval Yarom. RAMBleed: Reading Bits in Memory Without Accessing Them. In *S&P*, 2020.
- [113] Lucian Cojocar, Jeremie Kim, Minesh Patel, Lillian Tsai, Stefan Saroiu, Alec Wolman, and Onur Mutlu. Are We Susceptible to Rowhammer? An End-to-End Methodology for Cloud Providers. In *S&P*, 2020.
- [114] Zane Weissman, Thore Tiemann, Daniel Moghimi, Evan Custodio, Thomas Eisenbarth, and Berk Sunar. JackHammer: Efficient Rowhammer on Heterogeneous FPGA–CPU Platforms. *TCHES*, 2020.
- [115] Zhi Zhang, Yueqiang Cheng, Dongxi Liu, Surya Nepal, Zhi Wang, and Yuval Yarom. PTHammer: Cross-User-Kernel-Boundary Rowhammer Through Implicit Accesses. In *MICRO*, 2020.
- [116] Fan Yao, Adnan Siraj Rakin, and Deliang Fan. Deephammer: Depleting the Intelligence of Deep Neural Networks Through Targeted Chain of Bit Flips. In *USENIX Security*, 2020.
- [117] Finn de Ridder, Pietro Frigo, Emanuele Vannacci, Herbert Bos, Cristiano Giuffrida, and Kaveh Razavi. SMASH: Synchronized Many-Sided Rowhammer Attacks from JavaScript. In *USENIX Security*, 2021.
- [118] Patrick Jattke, Victor van der Veen, Pietro Frigo, Stijn Gunter, and Kaveh Razavi. Blacksmith: Scalable Rowhammering in the Frequency Domain. In *SP*, 2022.
- [119] M Caner Tol, Saad Islam, Berk Sunar, and Ziming Zhang. Toward Realistic Backdoor Injection Attacks on DNNs using RowHammer. arXiv:2110.07683v2 [cs.LG], 2022.
- [120] Andreas Kogler, Jonas Juffinger, Salman Qazi, Yoongu Kim, Moritz Lipp, Nicolas Boichat, Eric Shiu, Mattias Nissler, and Daniel Gruss. Half-Double: Hammering From the Next Row Over. In *USENIX Security*, 2022.
- [121] Lois Orosa, Ulrich Rührmair, A Giray Yağlıkcı, Haocong Luo, Ataberk Olgun, Patrick Jattke, Minesh Patel, Jeremie Kim, Kaveh Razavi, and Onur Mutlu. SpyHammer: Using RowHammer to Remotely Spy on Temperature. *IEEE Access*, 2024.
- [122] Zhi Zhang, Wei He, Yueqiang Cheng, Wenhao Wang, Yansong Gao, Dongxi Liu, Kang Li, Surya Nepal, Anmin Fu, and Yi Zou. Implicit Hammer: Cross-Privilege-Boundary Rowhammer through Implicit Accesses. *TDSC*, 2022.
- [123] Liang Liu, Yanan Guo, Yueqiang Cheng, Youtao Zhang, and Jun Yang. Generating Robust DNN with Resistance to Bit-Flip Based Adversarial Weight Attack. *TC*, 2022.
- [124] Yaakov Cohen, Kevin Sam Tharayil, Arie Haenel, Daniel Genkin, Angelos D Keromytis, Yossi Oren, and Yuval Yarom. HammerScope: Observing DRAM Power Consumption Using Rowhammer. In *CCS*, 2022.
- [125] Mengxin Zheng, Qian Lou, and Lei Jiang. TrojViT: Trojan Insertion in Vision Transformers. *CVPR*, 2023.
- [126] Michael Fahr Jr, Hunter Kippen, Andrew Kwong, Thinh Dang, Jacob Lichtinger, Dana Dachman-Soled, Daniel Genkin, Alexander Nelson, Ray Perlner, Arkady Yerukhimovich, et al. When Frodo Flips: End-to-End Key Recovery on FrodoKEM via Rowhammer. *CCS*, 2022.
- [127] Youssef Tobah, Andrew Kwong, Ingab Kang, Daniel Genkin, and Kang G. Shin. SpecHammer: Combining Spectre and Rowhammer for New Speculative Attacks. In *SP*, 2022.
- [128] Adnan Siraj Rakin, Md Hafizul Islam Chowdhury, Fan Yao, and Deliang Fan. DeepSteal: Advanced Model Extractions Leveraging Efficient Weight Stealing in Memories. In *SP*, 2022.
- [129] Kyungbae Park, Donghyuk Yun, and Sanghyeon Baeg. Statistical Distributions of Row-Hammering Induced Failures in DDR3 Components. *Microelectronics Reliability*, 2016.
- [130] Kyungbae Park, Chulseung Lim, Donghyuk Yun, and Sanghyeon Baeg. Experiments and Root Cause Analysis for Active-Precharge Hammering Fault in DDR3 SDRAM under 3xnm Technology. *Microelectronics Reliability*, 2016.
- [131] Chulseung Lim, Kyungbae Park, and Sanghyeon Baeg. Active Precharge Hammering to Monitor Displacement Damage Using High-Energy Protons in 3x-nm SDRAM. *TNS*, 2017.
- [132] Donghyuk Yun, Myungsang Park, Chulseung Lim, and Sanghyeon Baeg. Study of TID Effects on One Row Hammering using Gamma in DDR4 SDRAMs. In *IRPS*, 2018.
- [133] Thomas Yang and Xi-Wei Lin. Trap-Assisted DRAM Row Hammer Effect. *EDL*, 2019.
- [134] Andrew J. Walker, Sungkwon Lee, and Dafna Beery. On DRAM RowHammer and the Physics on Insecurity. *IEEE TED*, 2021.
- [135] Jeremie S. Kim, Minesh Patel, Abdullah Giray Yağlıkcı, Hasan Hassan, Roknoddin Azizi, Lois Orosa, and Onur Mutlu. Revisiting RowHammer: An Experimental Analysis of Modern Devices and Mitigation Techniques. In *ISCA*, 2020.
- [136] Lois Orosa, A Giray Yağlıkcı, Haocong Luo, Ataberk Olgun, Jisung Park, Hasan Hassan, Minesh Patel, Jeremie S. Kim, and Onur Mutlu. A Deeper Look into RowHammer’s Sensitivities: Experimental Analysis of Real DRAM Chips and Implications on Future Attacks and Defenses. In *MICRO*, 2021.
- [137] A. Giray Yağlıkcı, Haocong Luo, Geraldo F De Oliveira, Ataberk Olgun, Minesh Patel, Jisung Park, Hasan Hassan, Jeremie S Kim, Lois Orosa, and Onur Mutlu. Understanding RowHammer Under Reduced Wordline Voltage: An Experimental Study Using Real DRAM Devices. In *DSN*, 2022.
- [138] Mohammad Nasim Imtiaz Khan and Swaroop Ghosh. Analysis of Row Hammer Attack on STTRAM. In *ICCD*, 2018.
- [139] S. Agarwal, H. Dixit, D. Datta, M. Tran, D. Houssameddine, D. Shum, and F. Benistant. Rowhammer for Spin Torque Based Memory: Problem or Not? In *INTERMAG*, 2018.
- [140] Haitong Li, Hong-Yu Chen, Zhe Chen, Bing Chen, Rui Liu, Gang Qiu, Peng Huang, Feifei Zhang, Zizhen Jiang, Bin Gao, Lifeng Liu, Xiaoyan Liu, Shimeng Yu, H.-S. Philip Wong, and Jinfeng Kang. Write Disturb Analyses on Half-Selected Cells of Cross-Point RRAM Arrays. In *IRPS*, 2014.
- [141] Kai Ni, Xueqing Li, Jeffrey A. Smith, Matthew Jerry, and Suman Datta. Write Disturb in Ferroelectric FETs and Its Implication for 1T-FeFET AND Memory Arrays. *IEEE EDL*, 2018.
- [142] Paul R. Gensler, Victor M. van Santen, Jörg Henkel, and Hussam Amrouch. On the Reliability of FeFET On-Chip Memory. *TC*, 2022.
- [143] Haocong Luo, Ataberk Olgun, Abdullah Giray Yağlıkcı, Yahya Can Tuğrul, Steve Rhyner, Meryem Banu Cavlak, Joël Lindegger, Mohammad Sadrosadati, and Onur Mutlu. RowPress: Amplifying Read Disturbance in Modern DRAM Chips. In *ISCA*, 2023.
- [144] JEDEC. *JESD79-5c: DDR5 SDRAM Standard*, 2024.
- [145] Seyed Mohammad Seyedzadeh, Alex K. Jones, and Rami Melhem. Counter-Based Tree Structure for Row Hammering Mitigation in DRAM. *CAL*, 2017.
- [146] S. M. Seyedzadeh, A. K. Jones, and R. Melhem. Mitigating Wordline Crosstalk Using Adaptive Trees of Counters. In *ISCA*, 2018.
- [147] A. Giray Yağlıkcı, Jeremie S. Kim, Fabrice Devaux, and Onur Mutlu. Security Analysis of the Silver Bullet Technique for RowHammer Prevention. arXiv:2106.07084 [cs.CR], 2021.
- [148] JEDEC. *JESD79-5: DDR5 SDRAM Standard*, 2020.
- [149] Stefan Saroiu. DDR5 Spec Update Has All It Needs to End Rowhammer: Will It? <https://stefan.t8k2.com/rh/PRAC/index.html>.
- [150] Hasan Hassan, Ataberk Olgun, A. Giray Yağlıkcı, Haocong Luo, and Onur Mutlu. Self-Managing DRAM: A Low-Cost Framework for Enabling Autonomous and Efficient DRAM Maintenance Operations. In *MICRO*, 2024.
- [151] Haocong Luo, Yahya Can Tuğrul, F. Nisa Bostancı, Ataberk Olgun, A. Giray Yağlıkcı, and Onur Mutlu. Ramulator 2.0: A Modern, Modular, and Extensible DRAM Simulator. *CAL*, 2023.
- [152] SAFARI Research Group. Ramulator V2.0. <https://github.com/CMU-SAFARI/ramulator2>.
- [153] Fritz Graf. *Greek Mythology: An Introduction*. JHU Press, 1993.
- [154] SAFARI Research Group. Chronus. <https://github.com/CMU-SAFARI/Chronus>.
- [155] JEDEC. *JESD79-5: DDR5 SDRAM Standard*, 2020.
- [156] JEDEC. *JESD79-4C: DDR4 SDRAM Standard*, 2020.
- [157] Yoongu Kim, Vivek Seshadri, Donghyuk Lee, Jamie Liu, Onur Mutlu, Yoongu Kim, Vivek Seshadri, Donghyuk Lee, Jamie Liu, and Onur Mutlu. A Case for Exploiting Subarray-Level Parallelism (SALP) in DRAM. In *ISCA*, 2012.
- [158] Donghyuk Lee, Yoongu Kim, Vivek Seshadri, Jamie Liu, Lavanya Subramanian, and Onur Mutlu. Tiered-Latency DRAM: A Low Latency and Low Cost DRAM Architecture. In *HPCA*, 2013.
- [159] Donghyuk Lee, Yoongu Kim, Gennady Pekhimenko, Samira Khan, Vivek Seshadri, Kevin Chang, and Onur Mutlu. Adaptive-Latency DRAM: Optimizing DRAM Timing for the Common-Case. In *HPCA*, 2015.
- [160] Michael Redeker, Bruce F Cockburn, and Duncan G Elliott. An Investigation into Crosstalk Noise in DRAM Structures. In *MTDT*, 2002.
- [161] Kyungbae Park, Sanghyeon Baeg, Shi-Jie Wen, and Richard Wong. Active-Precharge Hammering on a Row-Induced Failure in DDR3 SDRAMs Under 3x nm Technology. In *IIRW*, 2014.
- [162] Chulseung Lim, Kyungbae Park, Geunyoung Bak, Donghyuk Yun, Myungsang Park, Sanghyeon Baeg, Shi-Jie Wen, and Richard Wong. Study of Proton Radiation Effect to Row Hammer Fault in DDR4 SDRAMs. *Microelectronics Reliability*, 2018.
- [163] Yichen Jiang, Huifeng Zhu, Dean Sullivan, Xiaolong Guo, Xuan Zhang, and Yier Jin. Quantifying RowHammer Vulnerability for DRAM Security. In *DAC*, 2021.
- [164] Wei He, Zhi Zhang, Yueqiang Cheng, Wenhao Wang, Wei Song, Yansong Gao, Qifei Zhang, Kang Li, Dongxi Liu, and Surya Nepal. WhistleBlower: A System-level Empirical Study on RowHammer. *TC*, 2023.
- [165] Sanghyeon Baeg, Donghyuk Yun, Myungsun Chun, and Shi-Jie Wen. Estimation of the Trap Energy Characteristics of Row Hammer-Affected Cells in Gamma-Irradiated DDR4 DRAM. *IEEE TNS*, 2022.
- [166] Onur Mutlu. RowHammer. Top Picks in Hardware and Embedded Security, 2018.
- [167] Ataberk Olgun, Majd Osseiran, Abdullah Giray Yağlıkcı, Yahya Can Tuğrul, Haocong Luo, Steve Rhyner, Behzad Salami, Juan Gomez Luna, and Onur Mutlu. An Experimental Analysis of RowHammer in HBM2 DRAM Chips. In *DSN Disrupt*, 2023.
- [168] Ataberk Olgun, Hasan Hassan, A. Giray Yağlıkcı, Yahya Can Tuğrul, Lois Orosa,

- Haocong Luo, Minesh Patel, Ergin Oğuz, and Onur Mutlu. DRAM Bender: An Extensible and Versatile FPGA-Based Infrastructure to Easily Test State-of-the-Art DRAM Chips. *TCAD*, 2023.
- [169] Longda Zhou, Jie Li, Zheng Qiao, Pengpeng Ren, Zixuan Sun, Jianping Wang, Blacksmith Wu, Zhigang Ji, Runsheng Wang, Kanyu Cao, and Ru Huang. Double-sided Row Hammer Effect in Sub-20 nm DRAM: Physical Mechanism, Key Features and Mitigation. In *IRPS*, 2023.
- [170] Zhenrong Lang, Patrick Jattke, Michele Marazzi, and Kaveh Razavi. BLASTER: Characterizing the Blast Radius of Rowhammer. *DRAMSec*, 2023.
- [171] Seungmin Baek, Minbok Wi, Seonyong Park, Hwayong Nam, Michael Jaemin Kim, Nam Sung Kim, and Jung Ho Ahn. Marionette: A rowhammer attack via row coupling. In *ASPLOS*, 2025.
- [172] Hewlett-Packard Enterprise. HP Moonshot Component Pack V2015.05.0, 2015.
- [173] Lenovo Group Ltd. Row Hammer Privilege Escalation. https://support.lenovo.com/us/en/product_security/row_hammer, 2015.
- [174] Seungki Hong, Dongha Kim, Jaehyung Lee, Reum Oh, Changsik Yoo, Sangjoon Hwang, and Jooyoung Lee. DSAC: Low-Cost Rowhammer Mitigation Using In-DRAM Stochastic and Approximate Counting Algorithm. arXiv:2302.03591 [cs.CR], 2023.
- [175] M. Marazzi, F. Solt, P. Jattke, K. Takashi, and K. Razavi. REGA: Scalable Rowhammer Mitigation with Refresh-Generating Activations. In *SP*, 2023.
- [176] Oğuzhan Canpolat, A Giray Yağlıkçı, Geraldo F Oliveira, Ataberk Olgun, Oğuz Ergin, and Onur Mutlu. Understanding the Security Benefits and Overheads of Emerging Industry Solutions to DRAM Read Disturbance. *DRAMSec*, 2024.
- [177] Kevin K Chang, Abhijith Kashyap, Hasan Hassan, Saugata Ghose, Kevin Hsieh, Donghyuk Lee, Tianshi Li, Gennady Pekhimenko, Samira Khan, and Onur Mutlu. Understanding Latency Variation in Modern DRAM Chips: Experimental Characterization, Analysis, and Optimization. In *SIGMETRICS*, 2016.
- [178] Kevin K Chang, A Giray Yağlıkçı, Saugata Ghose, Aditya Agrawal, Niladri Chatterjee, Abhijith Kashyap, Donghyuk Lee, Mike O'Connor, Hasan Hassan, and Onur Mutlu. Understanding Reduced-Voltage Operation in Modern DRAM Devices: Experimental Characterization, Analysis, and Mechanisms. In *SIGMETRICS*, 2017.
- [179] Kevin K Chang. *Understanding and Improving the Latency of DRAM-Based Memory Systems*. PhD thesis, Carnegie Mellon University, 2017.
- [180] Jeremie S Kim, Minesh Patel, Hasan Hassan, and Onur Mutlu. Solar-DRAM: Reducing DRAM Access Latency by Exploiting the Variation in Local Bitlines. In *ICCD*, 2018.
- [181] Deepak M Mathew, Éder F Zulian, Matthias Jung, Kira Kraft, Christian Weis, Bruce Jacob, and Norbert Wehn. Using Run-Time Reverse-Engineering to Optimize DRAM Refresh. In *MEMSYS*, 2017.
- [182] Yahya Can Tuğrul, A. Giray Yağlıkçı, İsmail Emir Yuksel, Oğuzhan Canpolat, Nisa Bostanci, Mohammad Sadrosadati, Oğuz Ergin, and Onur Mutlu. Understanding RowHammer Under Reduced Refresh Latency: Experimental Analysis of Real DRAM Chips and Implications on Future Solutions. In *HPCA*, 2025.
- [183] Ataberk Olgun, Majd Osseiran, Abdullah Giray Yağlıkçı, Yahya Can Tuğrul, Haocong Luo, Steve Rhyner, Behzad Salami, Juan Gomez Luna, and Onur Mutlu. Understanding Read Disturbance in High Bandwidth Memory: An Experimental Analysis of Real HBM2 DRAM Chips. arXiv:2310.14665 [cs.AR], 2023.
- [184] Ataberk Olgun, Majd Osseiran, A Giray Yağlıkçı, Yahya Can Tuğrul, Haocong Luo, Steve Rhyner, Behzad Salami, Juan Gomez Luna, and Onur Mutlu. Read Disturbance in High Bandwidth Memory: A Detailed Experimental Study on HBM2 DRAM Chips. In *DSN*, 2024.
- [185] Ranyang Zhou, Jacqueline Liu, Sabbir Ahmed, Nakul Kochar, Adnan Siraj Rakin, and Shaahin Angizi. Threshold Breaker: Can Counter-Based Rowhammer Prevention Mechanisms Truly Safeguard DRAM? arXiv:2311.16460 [cs.AR], 2023.
- [186] Ataberk Olgun, F. Nisa Bostanci, İsmail Emir Yuksel, Oğuzhan Canpolat, Haocong Luo, Geraldo F. Oliveira, A Giray Yağlıkçı, Minesh Patel, and Onur Mutlu. Variable Read Disturbance: An Experimental Analysis of Temporal Variation in DRAM Read Disturbance. In *HPCA*, 2025.
- [187] Yoongu Kim, Weikun Yang, and Onur Mutlu. Ramulator: A Fast and Extensible DRAM Simulator. *CAL*, 2016.
- [188] SAFARI Research Group. Ramulator — GitHub Repository. <https://github.com/CMU-SAFARI/ramulator>, 2021.
- [189] Stijn Eyerman and Lieven Eeckhout. System-Level Performance Metrics for Multi-program Workloads. *IEEE Micro*, 2008.
- [190] Allan Snively and Dean M Tullsen. Symbiotic Job Scheduling for A Simultaneous Multithreaded Processor. In *ASPLOS*, 2007.
- [191] Scott Rixner, William J. Dally, Ujval J. Kapasi, Peter Mattson, and John D. Owens. Memory Access Scheduling. In *ISCA*, 2000.
- [192] William K Zuravlev and Timothy Robinson. Controller for a Synchronous DRAM That Maximizes Throughput by Allowing Memory Requests and Commands to Be Issued Out of Order, 1997. U.S. Patent 5,630,096.
- [193] Onur Mutlu and Thomas Moscibroda. Stall-Time Fair Memory Access Scheduling for Chip Multiprocessors. In *MICRO*, 2007.
- [194] Dimitris Kaseridis, Jeffrey Stuecheli, and Lizy Kurian John. Minimalist Open-Page: A DRAM Page-Mode Scheduling Policy for the Many-Core Era. In *MICRO*, 2011.
- [195] Standard Perf. Eval. Corp. SPEC 2006. <http://www.spec.org/cpu2006/>, 2006.
- [196] Standard Perf. Eval. Corp. SPEC 2017. <http://www.spec.org/cpu2017/>, 2017.
- [197] Transaction Processing Performance Council. TPC Benchmarks. <http://tpc.org/>.
- [198] Jason E. Fritts, Frederick W. Steiling, Joseph A. Tucek, and Wayne Wolf. MediaBench II Video: Expediting the Next Generation of Video Systems Research. *MICPRO*, 2009.
- [199] Brian Cooper, Adam Silberstein, Erwin Tam, Raghu Ramakrishnan, and Russell Sears. Benchmarking Cloud Serving Systems with YCSB. In *SoCC*, 2010.
- [200] Kevin K Chang, Donghyuk Lee, Zeshan Chishti, Alaa R Alameldeen, Chris Wilkerson, Yoongu Kim, and Onur Mutlu. Improving DRAM Performance by Parallelizing Refreshes with Accesses. In *HPCA*, 2014.
- [201] İsmail Emir Yuksel, Yahya Can Tuğrul, Ataberk Olgun, F. Nisa Bostanci, A. Giray Yağlıkçı, Geraldo F. de Oliveira, Haocong Luo, Juan Gomez Luna, Mohammad Sadrosadati, and Onur Mutlu. Functionally-Complete Boolean Logic in Real DRAM Chips: Experimental Characterization and Analysis. In *HPCA*, 2024.
- [202] İsmail Emir Yuksel, Yahya Can Tuğrul, F. Bostanci, Geraldo F Oliveira, A Giray Yağlıkçı, Ataberk Olgun, Melina Soysal, Haocong Luo, Juan Gómez-Luna, Mohammad Sadrosadati, et al. Simultaneous Many-Row Activation in Off-the-Shelf DRAM Chips: Experimental Characterization and Analysis. In *DSN*, 2024.
- [203] Synopsys, Inc. Synopsys Design Compiler. <https://www.synopsys.com/implementation-and-signoff/>.
- [204] Rick Carter, J Mazurier, L Pirro, JU Sachse, P Baars, J Faul, C Grass, G Grasshoff, P Javorka, T Kammler, et al. 22nm FDSOI Technology for Emerging Mobile, Internet-of-Things, and RF Applications. In *IEDM*, 2016.
- [205] Yong-Bin Kim and T. Chen. Assessing Merged DRAM/Logic Technology. In *ISCA*, 1996.
- [206] Rajeev Balasubramanian, Andrew B. Kahng, Naveen Muralimanohar, Ali Shafiee, and Vaishnav Srinivas. CACTI 7: New Tools for Interconnect Exploration in Innovative Off-Chip Memories. *ACM TACO*, 2017.
- [207] Oğuzhan Canpolat, A Giray Yağlıkçı, Ataberk Olgun, İsmail Emir Yuksel, Yahya Can Tuğrul, Konstantinos Kanellopoulos, Oğuz Ergin, and Onur Mutlu. BreakHammer: Enhancing RowHammer Mitigations by Carefully Throttling Suspect Threads. *MICRO*, 2024.
- [208] Laurence Nagel and Donald O Pederson. SPICE (Simulation Program with Integrated Circuit Emphasis). 1973.
- [209] Jayadev Misra and David Gries. Finding Repeated Elements. *Science of Computer Programming*, 1982.
- [210] Karthik Chandrasekar, Benny Akesson, and Kees Goossens. Improved Power Modeling of DDR SDRAMs. In *DSD*, 2011.
- [211] Douglas G Altman and J Martin Bland. Standard Deviations and Standard Errors. *BMJ*, 2005.
- [212] Thomas Moscibroda and Onur Mutlu. Memory Performance Attacks: Denial of Memory Service in Multi-Core Systems. In *USENIX Security*, 2007.
- [213] Yoongu Kim, Michael Papamichael, Onur Mutlu, and Mor Harchol-Balder. Thread Cluster Memory Scheduling: Exploiting Differences in Memory Access Behavior. In *MICRO*, 2010.
- [214] Haocong Luo, İsmail Emir Yuksel, Ataberk Olgun, A Giray Yağlıkçı, Mohammad Sadrosadati, and Onur Mutlu. An Experimental Characterization of Combined RowHammer and RowPress Read Disturbance in Modern DRAM Chips. *DSN Disrupt*, 2024.
- [215] Kwangrae Kim, Jeonghyun Woo, Junsu Kim, and Ki-Seok Chung. HammerFilter: Robust Protection and Low Hardware Overhead Method for RowHammer. In *ICCD*, 2021.
- [216] Carsten Bock, Ferdinand Brasser, David Gens, Christopher Liebchen, and Ahmad-Reza Sadeghi. RIP-RH: Preventing Rowhammer-Based Inter-Process Attacks. In *ASIACCS*, 2019.
- [217] Zhi Zhang, Yueqiang Cheng, Dongxi Liu, Surya Nepal, and Zhi Wang. TeleHammer: A Stealthy Cross-Boundary Rowhammer Technique. arXiv:1912.03076 [cs.CR], 2019.
- [218] Timothy J Dell. A White Paper on the Benefits of Chipkill-Correct ECC for PC Server Main Memory. *IBM Microelectronics Division*, 1997.
- [219] Ruirui Huang and G. Edward Suh. IVEC: Off-Chip Memory Integrity Protection for Both Security and Reliability. In *ISCA*, 2010.
- [220] Gururaj Saileshwar, Prashant J. Nair, Prakash Ramrakhiani, Wendy Elsasser, and Moinuddin K. Qureshi. SYNERGY: Rethinking Secure-Memory Design for Error-Correcting Memories. In *HPCA*, 2018.
- [221] Long Chen and Zhao Zhang. MemGuard: A Low Cost and Energy Efficient Design to Support and Enhance Memory System Reliability. In *ISCA*, 2014.
- [222] Moinuddin Qureshi. Rethinking ECC in the Era of Row-Hammer. *DRAMSec*, 2021.
- [223] Oğuzhan Canpolat, A Giray Yağlıkçı, Geraldo F Oliveira, Ataberk Olgun, Nisa Bostanci, İsmail Emir Yuksel, Haocong Luo, Oğuz Ergin, and Onur Mutlu. Chronus: Understanding and securing the cutting-edge industry solutions to dram read disturbance. In *HPCA*, 2025.
- [224] Jumin Kim, Seungmin Baek, Minbok Wi, Hwayong Nam, Michael Jaemin Kim, Sukhan Lee, Kyomin Sohn, and Jung Ho Ahn. Per-row activation counting on real hardware: Demystifying performance overheads. *CAL*, 2025.
- [225] Onur Mutlu. Retrospective: Flipping Bits in Memory Without Accessing Them: An Experimental Study of DRAM Disturbance Errors. Retrospective Issue for ISCA-50, 2023.
- [226] Kenneth H. Rosen. *Discrete Mathematics and Its Applications*. McGraw-Hill Education, 8th edition, 2019.
- [227] Herbert B Enderton. *A mathematical introduction to logic*. Elsevier, 2001.
- [228] Sarabjeet Singh and Manu Awasthi. Memory centric characterization and analysis of spec cpu2017 suite. In *ICPE*, 2019.
- [229] Moinuddin Qureshi. Autorfm: Scaling low-cost in-dram trackers to ultra-low rowhammer thresholds. In *HPCA*, 2025.
- [230] Suhas Vittal, Salman Qazi, Poulami Das, and Moinuddin Qureshi. Mopac: Efficiently mitigating rowhammer with probabilistic activation counting. In *ISCA*, 2025.

A. Decrementer Circuit of Chronus

Chronus uses custom circuitry to update row activation counters. To do so, we implement a circuit that decrements an 8-bit number (i.e., size of a Chronus activation counter, as explained in §7) by 1. Table 3 shows the pseudo hardware description of the decrementer and the resources to implement the circuit. In the table, x and y respectively show the 8-bit row activation counter as input and 8-bit updated value as output of the circuit, where $y = x - 1$. The subscripted numbers denote the bit index of the input and the output, e.g., x_1 and y_1 respectively show the first bit of the 8-bit input and 8-bit output of the circuit. Rows of the table show 1) the logical expression to obtain each bit of y , 2) the logic gates needed to implement the expression, and 3) the number of transistors needed to implement the logic gates.

Table 3: Gate-level implementation of the circuitry that decrements an 8-bit number by 1

Logical expression	NOT	MUX	NAND	NOR	#Ts
$y_0 = \bar{x}_0$	1	0	0	0	2
$y_1 = x_0 \ ? \ x_1 : \bar{x}_1$	1	1	0	0	10
$y_2 = \text{nor}(x_0, x_1) \ ? \ \bar{x}_2 : x_2$	1	1	0	1	14
for $i = 3 \rightarrow 7$:					
$y_i = \text{nand}(y_{i-1}, \bar{x}_{i-1}) \ ? \ x_i : \bar{x}_i$	1	1	1	0	14
Total:	8	7	5	1	96

B. Artifact Appendix

B.1. Abstract

Our artifact contains the data, source code, and scripts needed to reproduce our results. We provide: 1) the source code of our simulation infrastructure based on Ramulator2 and 2) all evaluated memory access traces and all major evaluation results. We provide Bash and Python scripts to analyze and plot the results automatically.

B.2. Artifact Check-list (meta-information)

Parameter	Value
Program	C++ program Python3 scripts Shell scripts
Compilation	C++ compiler with c++20 features
Run-time environment	Ubuntu 20.04 (or similar) Linux C++20 build toolchain (tested with GCC 10) Python 3.10+ Podman 4.5+ Git
Metrics	Weighted speedup DRAM energy
Experiment workflow	Perform simulations, aggregate results, and run analysis scripts on the result
Experiment customization	Possible. See §B.6
Disk space requirement	$\approx 30\text{GiB}$
Workflow preparation time	≈ 30 minutes
Experiment completion time	≈ 1 day (on a compute cluster with 250 cores)
Publicly available?	Benchmarks (https://zenodo.org/record/14281771) Zenodo (https://zenodo.org/record/14741186) GitHub (https://github.com/CMU-SAFARI/Chronus)

B.3. Description

We highly recommend using Slurm with a cluster that can run experiments in bulk.

How To Access. Source code and scripts are available at <https://github.com/CMU-SAFARI/Chronus>.

Hardware Dependencies. We recommend using a PC with 32 GiB of main memory. Approximately 30 GiB of disk space is needed to store intermediate and final evaluation results.

Software Dependencies.

- GNU Make, CMake 3.20+
- C++20 build toolchain (tested with GCC 10)
- Python 3.9+
- pip: matplotlib, pandas, seaborn, pyyaml, wget, scipy
- Ubuntu 22.04
- (Optional) Slurm 20+
- (Optional) Podman 4.5+

Benchmarks. We use workload memory traces collected from SPEC2006, SPEC2017, TPC, MediaBench, and YCSB benchmark suites. These traces are available at <https://zenodo.org/records/14281771>. Install scripts will download and extract the traces.

B.4. Installation

The following steps will download and prepare the repository for the main experiments:

1. Clone the git repository.

```
$ git clone \
git@github.com:CMU-SAFARI/Chronus.git
```

2. (Optional) Build the Podman container to run the scripts.

```
$ podman build . -t chronus_artifact
```

The following command runs a script using the container:

```
$ podman run --rm -v $PWD:/app \
chronus_artifact <script>
```

3. Install Python dependencies, compile Ramulator2, download workload traces, and run a small sanity check.

```
$ ./run_simple_test.sh
```

B.5. Evaluation and Expected Results

Claim 1 (C1). Latest industry solutions to read disturbance induce prohibitively large system performance overhead for both modern (i.e., $N_{RH}=1\text{K}$) and future (i.e., $N_{RH}\leq 1\text{K}$) DRAM chips. This property is proven by evaluating the effect of state-of-the-art read disturbance mitigation mechanisms on system performance (E1) as described in §6 whose results are illustrated in Fig. 4.

Claim 2 (C2). Chronus outperforms both 1) state-of-the-art industry solutions to read disturbance (i.e., PRAC [144] and PRFM [148]) and 2) state-of-the-art academic solutions to RowHammer (i.e., Graphene [4], Hydra [24], and PARA [1]) in terms of system performance (Figs. 7, 8, and 9), DRAM energy (Fig. 10), and storage (Fig. 11). This property is proven by evaluating and comparing the impact of Chronus and prior state-of-the-art read disturbance mitigation mechanisms on system performance and DRAM energy on single-core and multi-core workloads (E2) as described in §9.

Experiments (E1 and E2). [Ramulator2 simulations] [10 human-minutes + 20 compute-hours (assuming ~ 500 Ramulator2 simulations run in parallel) + 30GiB disk]

We prove our claims in two steps: 1) Execute Ramulator2 simulations to generate data supporting C1 and C2; 2) Plot all figures that prove C1 and C2.

1. Launch all Ramulator2 simulation jobs.¹⁹

```
$ ./run_with_personalcomputer.sh
(or ./run_with_slurm.sh if Slurm is available)
```

2. Wait for the simulations to end. The following displays the status and generates scripts to restart failed runs:

```
$ ./check_run_status.sh
```

3. Parse simulation results and collect statistics.

```
$ ./parse_results.sh
```

4. Generate all figures that support C1 and C2.

```
$ ./plot_all_figures.sh
```

B.6. Experiment Customization

Our scripts provide easy configuration of the 1) evaluated read disturbance mitigation mechanisms, 2) tested read disturbance thresholds, 3) simulation duration, and 4) simulated workload combinations. The run parameters are configurable in `scripts/run_config.py` with 1) `mitigation_list`, 2) `tRH_list`, and 3) `NUM_EXPECTED_INSTS` or `NUM_MAX_CYCLES`, respectively. Simulated single-core and multi-core workload combinations can be updated in `mixes/hpcasingle.mix` and `mixes/hpcabenign.mix`, respectively.

B.7. Methodology

Submission, reviewing and badging methodology:

- <https://www.acm.org/publications/policies/artifact-review-and-badging-current>
- <https://cTuning.org/ae>

C. Comparison to ABACuS

We compare Chronus to ABACuS [33], a storage-optimized deterministic mechanism that uses the Misra-Gries frequent item counting algorithm [209] and maintains frequently accessed row counters completely within the memory controller. ABACuS makes a key observation that many workloads (both benign workloads and RowHammer attacks) tend to access DRAM rows with the same row address in multiple DRAM banks at *around the same time* because i) modern memory address mapping schemes interleave consecutive cache blocks across different banks and ii) workloads tend to access cache blocks in close proximity around the same time due to the spatial locality in their memory accesses [33]. ABACuS exploits this observation by maintaining a single counter across *all* banks instead of maintaining a counter *per* bank (e.g., [4, 32]). By doing so, ABACuS accurately tracks activation counts at significantly reduced area overhead [33]. We implement ABACuS

¹⁹Slurm job partition and the maximum number of jobs are configurable via the `AE_SLURM_PART_NAME` variable in `./run_with_slurm.sh` and `MAX_SLURM_JOBS` variable in `scripts/run_config.py`, respectively.

in Ramulator 2.0 [152, 154] and follow the same methodology in §9. We use the address mapping described in the ABACuS paper (see §9 of [33]) instead of RoBaRaCoCh used in §10.

System Performance. Fig. 12 presents the performance overheads of Chronus and ABACuS across 60 benign four-core workloads for N_{RH} values from 1K to 20. x and y axes respectively show the N_{RH} values and system performance in terms of weighted speedup normalized to a baseline with *no* read disturbance mitigation (higher y value is better). Each colored bar depicts the mean system performance of a mechanism across 60 four-core workloads and error bars show the standard error of the mean across 60 four-core workloads.

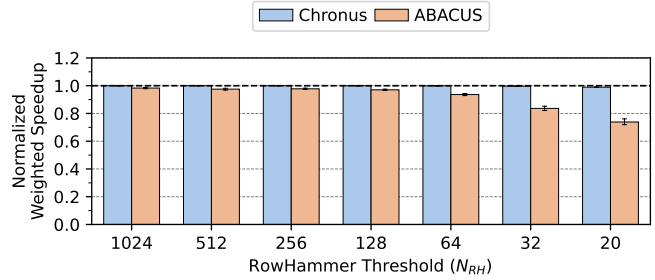


Figure 12: Performance impact of Chronus and ABACuS on 60 benign four-core workloads

We make three observations from Fig. 12. First, Chronus outperforms ABACuS across all evaluated N_{RH} values. Second, as N_{RH} decreases from 1K to 20, ABACuS’s performance overhead increases from 1.7% to 26.4%. In contrast, Chronus’s performance overhead increases from <0.1% to only 3.2%. Third, Chronus’s system performance overhead decreases with ABACuS’s address mapping. For example, at $N_{RH} = 20$, Chronus’s performance overhead decreases from 17.9% (shown in Fig. 8) to 3.2% when the address mapping changes from RoBaRaCoCh to ABACuS’s mapping. This is likely due to ABACuS’s mapping leading to a lower row conflict rate by better interleaving rows across banks.²⁰

Storage. Fig. 13 shows the storage overhead in MiB (y axis) of the evaluated read disturbance mitigation mechanisms as N_{RH} decreases (x axis). We evaluate the storage usage of Chronus (DRAM) and ABACuS (CAM+SRAM in CPU) as a function of N_{RH} for a DRAM module with 64 banks and 128K rows per bank.

We make two observations from Fig. 13. First, ABACuS’s storage overhead in CPU is significantly lower compared to Chronus’s storage overhead in DRAM. However, Chronus overhead is completely within the DRAM chip where the per-bit storage hardware complexity is relatively low. Second, as N_{RH}

²⁰Reduced row conflict rate in ABACuS’s mapping increases baseline system performance. When a read disturbance mitigation mechanism is present, the benefits can be further improved because DRAM rows are activated fewer times on average, and thus the mitigation mechanism can perform fewer preventive refreshes. We do *not* use ABACuS’s mapping in our main evaluation (§10) because each mapping differently affects different read disturbance mechanisms. For example, Hydra’s [24] system performance overhead significantly (>10%) increases with ABACuS’s mapping compared to RoBaRaCoCh (not shown). We leave a rigorous evaluation of the memory address mapping’s effect on different read disturbance mitigation mechanisms to future work.

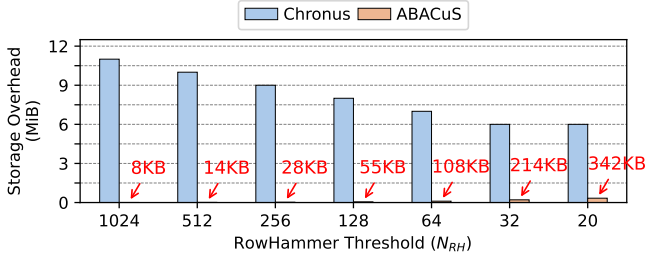


Figure 13: Storage used by Chronus (DRAM) and ABACuS (CAM+SRAM in CPU) as a function of RowHammer threshold for a DRAM module with 64 banks and 128K rows per bank

decreases from 1K to 20, ABACuS’s storage overhead in CPU increases from 8KB to 324KB. This is because as N_{RH} decreases, ABACuS needs to track many more rows and thereby requires more counters (implemented as CAM and SRAM).

D. Worst-Case Access Pattern Analysis

We prove that the access pattern used in §11 yields the maximum theoretical DRAM bandwidth consumption of preventive refreshes in a Chronus- or PRAC-protected system.

Properties. We build our proof on three properties of PRAC and Chronus: *P1*) a row’s activation count increases by one when the row is opened and closed; *P2*) a back-off is triggered when a row’s activation count reaches N_{BO} ; *P3*) a back-off refreshes *i*) N_{Ref} rows with the highest activation count in PRAC and *ii*) all rows that exceed N_{BO} in Chronus for each bank.

Maximum Bandwidth Consumption of Preventive Refreshes. For a given access pattern, we calculate the fraction of DRAM bandwidth consumed for performing preventive refreshes. Our *DRAM Bandwidth Consumption (DBC)* function is formally defined as $DBC: P \rightarrow [0, 1]$, where P denotes the set of all possible access patterns and $[0, 1]$ is the fraction of DRAM bandwidth consumed by preventive refreshes. For example, the worst-case access pattern evaluated in §11 triggers a preventive refresh operation N_{Ref} times and each refresh operation takes t_{RFM} (i.e., $N_{Ref} \times t_{RFM}$). To trigger a refresh, this access pattern includes N_{BO} row activations, each of which takes at least t_{RC} (i.e., $N_{BO} \times t_{RC}$). As such, the adversarial pattern evaluated in §11 (i.e., P_{ADV}) has the DRAM bandwidth consumption presented in Expression 3.

$$DBC(P_{ADV}) = \frac{(N_{Ref} \times t_{RFM})}{(N_{Ref} \times t_{RFM}) + (N_{BO} \times t_{RC})} \quad (3)$$

Proof Overview. We prove that P_{ADV} yields the maximum DRAM bandwidth consumption in four steps using proof-by-contradiction [226]. First, we assume that there exists an adversarial pattern P_{HYP} (i.e., hypothetical adversarial pattern) that yields a greater DRAM bandwidth consumption than P_{ADV} within an arbitrary time window T .²¹ Second, we calculate the number of back-offs triggered by P_{ADV} within T as a lower bound for P_{HYP} . Third, we calculate the time needed to perform the preventive refreshes of back-offs caused by P_{HYP} . Fourth,

²¹We choose an arbitrary T with no assumptions. Therefore, the following steps of the proof apply for all T by the *Universal Introduction* rule [227].

we show that time remaining after P_{HYP} ’s preventive refreshes *cannot* be used to trigger P_{HYP} ’s back-offs within T . Therefore, a pattern that yields greater DRAM bandwidth availability *cannot* exist within the constraints of PRAC and Chronus.

Step 1: Adversarial memory access pattern. Assume there exists an adversarial access pattern P_{HYP} that yields a greater DRAM bandwidth consumption than P_{ADV} within an arbitrary time window T (i.e., $DBC(P_{HYP}) > DBC(P_{ADV})$). Since P_{HYP} consumes more DRAM bandwidth than P_{ADV} , P_{HYP} must trigger at least one more back-off than P_{ADV} . For a given access pattern P , we calculate the *Back-Offs Triggered (BOT)* within a time window of length T . To do so, we find the DRAM bandwidth consumed by access pattern P (i.e., $T \times DBC(P)$) and divide it by the duration of a back-off (i.e., $N_{Ref} \times t_{RFM}$) as shown in Expression 4.

$$BOT(P, T) = T \times DBC(P) / (N_{Ref} \times t_{RFM}) \quad (4)$$

Step 2: Lower bound of the number of back-offs. Based on the assumption in Step 1, $BOT(P_{HYP}, T)$ should be larger than $BOT(P_{ADV}, T)$. By placing Expressions 3 and 4 in the restriction $BOT(P_{HYP}, T) > BOT(P_{ADV}, T)$, we derive Expression 5.

$$BOT(P_{HYP}, T) > \frac{T}{N_{Ref} \times t_{RFM} + N_{BO} \times t_{RC}} \quad (5)$$

Step 3: Time taken to perform preventive refreshes. By knowing the lower bound for the number of back-offs triggered by P_{HYP} , we calculate the time taken to perform the preventive refreshes of P_{HYP} ’s back-offs (i.e., PR_{HYP}) by multiplying the number of back-offs (i.e., $BOT(P_{HYP}, T)$) with the duration of a back-off (i.e., $N_{Ref} \times t_{RFM}$) in Expression 6.

$$PR_{HYP} > \frac{T \times N_{Ref} \times t_{RFM}}{N_{Ref} \times t_{RFM} + N_{BO} \times t_{RC}} \quad (6)$$

Step 4: Remaining time after the preventive refreshes. The time taken to both trigger and perform the preventive refreshes of P_{HYP} should fit within T . We calculate the remaining time after performing the preventive refreshes of P_{HYP} ’s back-offs (i.e., RT_{HYP}). Expression 6 provides a lower bound for PR_{HYP} . Therefore, subtracting PR_{HYP} from T yields an upper bound for RT_{HYP} (i.e., $RT_{HYP} < T - PR_{HYP}$). Solving this expression for RT_{HYP} , we derive Expression 7.

$$RT_{HYP} < \frac{T \times N_{BO} \times t_{RC}}{N_{Ref} \times t_{RFM} + N_{BO} \times t_{RC}} \quad (7)$$

Triggering a back-off with a single bank takes $N_{BO} \times t_{RC}$ (following from *P1* and *P2*) and concurrent aggressors *cannot* be used to trigger a back-off more quickly (following from *P3*). Given *P1*, *P2*, and *P3*, we calculate time needed to trigger P_{HYP} ’s back-offs in a PRAC or Chronus protected system (TBO_{HYP}). Expression 5 presents a lower bound for $BOT(P_{HYP}, T)$. Multiplying $BOT(P_{HYP}, T)$ with the time taken to trigger a single back-off yields a lower bound for TBO_{HYP} (i.e., $TBO_{HYP} > BOT(P_{HYP}, T) \times N_{BO} \times t_{RC}$). Solving this expression for TBO_{HYP} , we evaluate Expression 8.

$$TBO_{HYP} > \frac{T \times N_{BO} \times t_{RC}}{N_{Ref} \times t_{RFM} + N_{BO} \times t_{RC}} \quad (8)$$

By comparing Expressions 7 and 8, we see that the time necessary to trigger P_{HYP} 's preventive refreshes (TBO_{HYP}) exceeds the time remaining after P_{HYP} 's preventive refreshes are performed (RT_{HYP}), i.e., $RT_{HYP} < TBO_{HYP}$. This means that *no* P_{HYP} exists that obey the three properties of PRAC and Chronus (i.e., $P1$, $P2$, and $P3$). Therefore, P_{ADV} (as used in §11) yields the maximum DRAM bandwidth consumption, and thus represents the worst possible access pattern.

E. Errata and New Results

A new study [224] pointed out a bug where the t_{RAS} , t_{RTP} , and t_{WR} DRAM timing parameters for PRAC-enabled systems were *not* being reduced correctly in the evaluations of our paper's previous version [223]. We thank the authors of [224] for providing us with the feedback. We fixed the bug, and updated all affected results and figures in this version of our paper. All results presented in this paper are collected with the bug fix included. We also updated Chronus' open-source repository [154] with the bug fix.

We now evaluate the effect the bug fix had on the performance and energy overheads of PRAC. Table 4 presents how the bug has changed the system performance and DRAM energy overheads of PRAC in our evaluations (see §6 and §10 for all results with the bug fix). Columns labeled as *Old* and *New* respectively present 1) the results with the bug in the previous version of the paper [223] and 2) the results after fixing the bug in this current version of the paper. We report that the difference in PRAC's results *after* the bug fix is *not significant enough* to change *any* of our claims or conclusions in this work (or the previous version [223]).

Table 4: Changes in Four-Core Results for PRAC Performance and Energy Overheads After Fixing the Bug. Old: Results with the bug (previous version of the paper [223]). New: Results after fixing the bug (this current version of the paper).

N_{RH}	Single-Core Perf. Overhead		Four-Core Perf. Overhead		Four-Core Energy Overhead	
	Old	New	Old	New	Old	New
1K	22.0%	14.0%	9.7%	5.8%	18.4%	10.7%
512	22.0%	14.0%	9.7%	5.8%	18.4%	10.7%
256	22.1%	14.1%	9.7%	5.9%	18.5%	10.8%
128	22.3%	14.4%	9.9%	6.1%	18.6%	10.9%
64	26.2%	19.1%	11.7%	8.1%	20.4%	12.8%
32	46.1%	42.5%	30.4%	29.1%	48.0%	40.8%
20	90.9%	90.3%	81.2%	78.5%	6.9x	6.6x

From Table 4, we observe that the bug caused a smaller overhead difference at low N_{RH} values (e.g., <128) compared to high N_{RH} values (e.g., $=1K$). This is because PRAC causes more back-offs as N_{RH} decreases and those back-offs dominate PRAC's performance overhead. As a result, the effect of increased precharge and row cycle latencies on performance degradation become less significant.

The mentioned recent study [224] further argues that PRAC's system performance overhead on real hardware is lower than what our simulations show. We identify two key methodological differences between our study and [224] that cause the lower PRAC performance impact. First, [224] evaluates a

relatively small set of homogeneous workloads (i.e., only 23 SPEC 2017 workloads with mostly low memory-intensity) compared to our 60 heterogeneous workloads with varying memory intensities chosen from five major benchmark suites (SPEC CPU2006 [195], SPEC CPU2017 [196], TPC [197], MediaBench [198], and YCSB [199], see §6). Second, [224] evaluates systems with much larger caches. For example, the last-level caches of systems in [224] is 4.5x larger than our simulated system (see §6). The increased cache size makes SPEC 2017 workloads mostly cache-resident [228]. Therefore, PRAC does *not* induce performance overhead on a system that is *not* bottlenecked by memory. In contrast, our simulation methodology implements smaller caches as a best-effort to account for memory-bottlenecked systems which is standard practice in literature (see, e.g., [3, 4, 8, 12, 17, 18, 24, 32, 33, 35, 37, 135, 175, 229, 230]), using publicly available well-established benchmark suites.

We now experimentally demonstrate that these two methodological choices lead to the discrepancy in PRAC's performance overheads between our work and [224]. To do so, we repeat our simulation-based evaluation using the *same* system configuration and *same* workloads used in [224]. Fig. 14 presents the performance overhead of PRAC across 23 eight-core homogeneous SPEC 2017 workloads for N_{RH} values from 1K to 20 (these are the same 23 workloads evaluated in [224]). x and y axes respectively show the N_{RH} values and performance in terms of weighted speedup normalized to a baseline with *no* read disturbance mitigation (higher y value is better). Each bar depicts the geomean system performance of PRAC-4 across 23 eight-core workloads and error bars show the 100% confidence interval across 23 eight-core workloads.

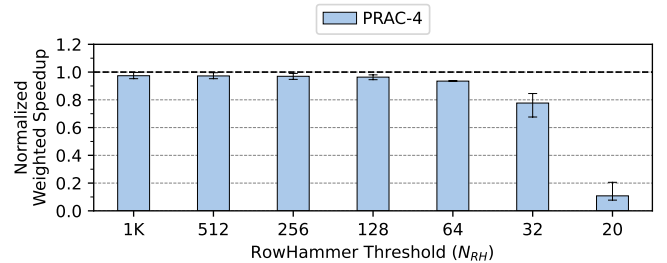


Figure 14: Performance impact of PRAC on 23 eight-core homogeneous SPEC 2017 workloads, normalized to a baseline with *no* read disturbance mitigation

We make two observations from Fig. 14. First, at $N_{RH} = 1K$, PRAC-4 induces an average (maximum) system performance overhead of 2.4% (4.6%), which is similar to the average (maximum) numbers of 1.3% (3.8%) reported in [224] for a similarly configured real system. Second, when N_{RH} decreases from 1K to 20, PRAC-4's average (maximum) system performance overhead increases to 78.8% (85.9%). Kim et al.'s real system-based evaluation methodology limits their tests to *only* an N_{RH} value of 1K. Therefore, we *cannot* compare our simulation results for sub-1K N_{RH} values against [224].

We conclude that the discrepancy in PRAC's performance impact across our work and [224] is very likely an artifact of [224] adopting a different system configuration and different work-

loads, as opposed to simulation-based evaluations that “often fall short of accurately modeling the performance characteristics of real-world memory systems” (as claimed very generally by [224] without providing commensurate evidence).

We also evaluate the DRAM energy overhead of PRAC using the DRAMPower [210] integration of Ramulator 2.0 under the *same* system configuration and *same* workloads used in [224]. Fig. 15 presents the energy consumption of PRAC across 23 eight-core homogeneous SPEC 2017 workloads for N_{RH} values from 1K to 20. x and y axes respectively show the N_{RH} values and energy consumption normalized to a baseline with *no* read disturbance mitigation (lower y value is better). Each bar depicts the geomean energy consumption of PRAC-4 across 23 eight-core workloads and error bars show the 100% confidence interval across 23 eight-core workloads.

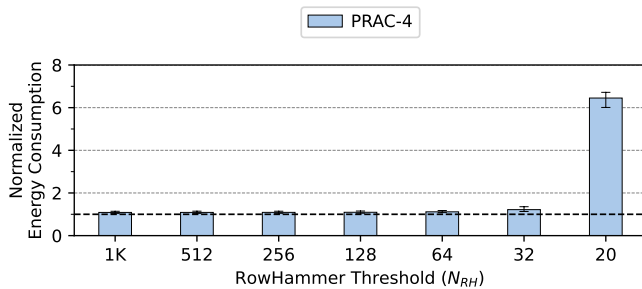


Figure 15: DRAM energy impact of PRAC on 23 eight-core homogeneous SPEC 2017 workloads, normalized to a baseline with *no* read disturbance mitigation

We make two observations from Fig. 15. First, at $N_{RH} = 1K$, PRAC-4 induces an average (maximum) energy consumption overhead of 8.9% (14.1%). Second, when N_{RH} decreases from 1K to 20, PRAC-4’s average (maximum) energy consumption overhead increases to 5.46x (5.72x). We *cannot* compare our simulation results values against [224] because Kim et al.’s real system-based study does *not* include energy evaluations.

We conclude that PRAC’s energy overhead is 1) non-negligible ($\geq 8\%$) at high N_{RH} values (i.e., $N_{RH} = 1K$) and 2) prohibitively large ($\geq 5x$) at low N_{RH} values (i.e., $N_{RH} < 32$) even under system configuration and workload combinations that observe relatively lower PRAC system performance overhead (e.g., [224]).